THERMOHYDRAULICS ANALYSIS OF THE UNIVERSITY OF UTAH TRIGA REACTOR OF HIGHER POWER DESIGNS

by

Philip Marcus Babitz

A thesis submitted to the faculty of
The University of Utah
in partial fulfillment of the requirements for the degree of

Master of Science

in

Nuclear Engineering

Department of Civil and Environmental Engineering

The University of Utah

December 2012

The University of Utah Graduate School

STATEMENT OF THESIS APPROVAL

The thesis of **Philip Marcus Babitz**

has been approved by the following supervisory committee members:

Tatjana Jevremovic	, Chair	**10/16/12** Date Approved
Dong-Ok Choe	, Member	**10/16/12** Date Approved
Haori Yang	, Member	**10/16/12** Date Approved

and by **Chris Pantelides** , Chair of

the Department of **Civil and Environmental Engineering**

and by Charles A. Wight, Dean of The Graduate School.

ABSTRACT

The natural convective flow conditions of the University of Utah TRIGA Reactor (UUTR) were simulated using SolidWorks Flow Simulation, Ansys Fluent and PARET-ANL. The simulations were run at UUTR's maximum operating power of 90 kW and at theoretical higher powers to analyze the thermohydraulics aspects of increasing the reactor's power in determining a design basis for higher power including the cost estimate. It was found that the natural convection current becomes much more pronounced at higher power levels with vortex shedding also occurring. A departure from nucleate boiling analysis showed that while nucleate boiling begins near 210 kW it remains in this state and does not approach the critical heat flux at powers up to 500 kW. Two upgrades are proposed for extended operations: $5,000 to offer extended runtimes up to 150 kW and a theoretical, replacement cooling system with materials estimated at $180,000.

CONTENTS

LIST OF TABLES

ACKNOWLEDGEMENTS

I wish to thank my advisor Dr. Tatjana Jevremovic for her great encouragement, guidance and assistance in helping me to complete my thesis. I am also very grateful to Dr. Dong-Ok Choe and Dr. Haori Yang for their assistance and willingness to help with my research. In addition, I would like to thank my fellow graduate students Avdo Cutic, Todd Sherman and Jason Rapich for their help and friendship.

This thesis would not have been possible without the help of my grandfather, Richard Schanz, who encouraged me to pursue a master's degree. Also, I am especially grateful for the support of all my family and my loving wife, Jane.

CHAPTER 1

INTRODUCTION

1.1 Thesis Objectives

The University of Utah is home to a TRIGA reactor (UUTR) currently licensed to operate up to 100 kW. The objective of this thesis is to analyze the thermohydraulics aspect of increasing the reactor's power in determining a design basis area for higher power including the cost estimate. A survey of research reactors and their cooling systems is conducted and reactor pool conditions are modeled using SolidWorks Flow Simulation, PARET-ANL and Ansys Fluent. These results form a basis for the reactor's power upgrade and the design of its cooling system.

1.2 Background

The University of Utah TRIGA Reactor has been operating since 1975 without an incident. The UUTR is a modified TRIGA Mark I pool-type reactor that currently is operated at a maximum of 90 kW, although licensed to operate at a maximum power of 100 kW. However, the fuel core design has the potential of increasing the overall power up to 1 MW.

The reactor is located on the first floor of the Merrill Engineering Building at the University of Utah lower campus. The reactor core is immersed into a deep

tank filled with purified water and is mounted a small distance off the bottom of the vessel. The water in the reactor tank provides cooling, a biological shield and neutron moderation. The core is of hexagonal shape. Inside the core are rings containing spaces for fuel or other elements and allowing water to flow. Surrounding the outside of the aluminum tank vessel is a larger diameter, steel vessel filled with sand that provides a 2 foot (0.61 meter) barrier between the two vessels [1]. Figure 1-1 provides a side view of the reactor layout.

The UUTR is operated by trained and NRC licensed staff and students of the University of Utah Nuclear Engineering Program. The UUTR is utilized in many ways: to train students on reactor operation and nuclear principles, it provides a neutron and gamma source for research and is used for neutron activation analysis. The reactor is as well a major research and community outreach tool; tours of the facility are conducted educating the public and younger students about nuclear engineering.

1.3 Current Configuration

The current 100 kW UUTR is cooled using only natural convection. The reactor pool is filled with deionized water and holds 8,100 gallons of water when full. When the reactor is operated the heat generated dissipates directly into the pool water. A primary loop is present off the main pool that deionizes the water and contains a small cooling system. This loop is driven by an Ingersol-Rand 1-1/2 hp centrifugal pump creating a 4-6 gpm flow rate. A diagram of the primary loop is shown in Figure 1-2. Under normal operating conditions, half of the flow is diverted from the primary loop to pass through the deionizing system. The deionizer consists of two mixed resin beds: a rough cut bed to treat the make-up

water and a fine cut bed to treat the water through the primary loop. The remaining, un-treated half of the primary loop's water travels through the, normally inoperative, cooling system's heat exchanger and back into the reactor pool.

The cooling system is a Dunham-Bush R-134 based compressor and heat exchanger/evaporator rated to 25 kW of cooling load. When activated the compressor pumps the liquid R-134 into the heat exchanger where it evaporates and cools the fluid being pumped through the primary loop. However, this system is rarely used since it is undersized and there is a danger of the refrigerant freezing the water in the primary loop if the water is not moving through the loop at sufficient speed. Normally, the reactor is only operated intermittently (1-2 times per week) and cooling is accomplished through ambient heat transfer to the surroundings.

1.4 Survey of Research Reactors

As of this writing there are 30 research and test reactors operating in the United States [2]. A list of these reactors, their locations and power levels are all shown in Table 1-1. A visual representation of the reactors, categorized by their licensed operating power, is shown in Figure 1-3. Among TRIGA type reactors UUTR is one of the lowest powered operating.

Of this group of research reactors powered 1 kW and greater, only three rely primarily on natural, ambient heat transfer for cooling. The remaining reactors are equipped with forced convection systems of equal or greater cooling load to the reactor's licensed power level. The most common type of system used was a dual loop heat exchanger linked to a cooling tower in the outside environment.

1.5 Motivation

Thermodynamic calculations and CFD (Computational Fluid Dynamics) simulations were performed to gain a better understanding of heat flow in the UUTR water tank. These analyses are necessary to study the feasibility of a power upgrade for UUTR. The results will help to determine a theoretical, new higher power level for UUTR and to design a proper forced convection cooling system that will allow extended reactor operations at the new power level.

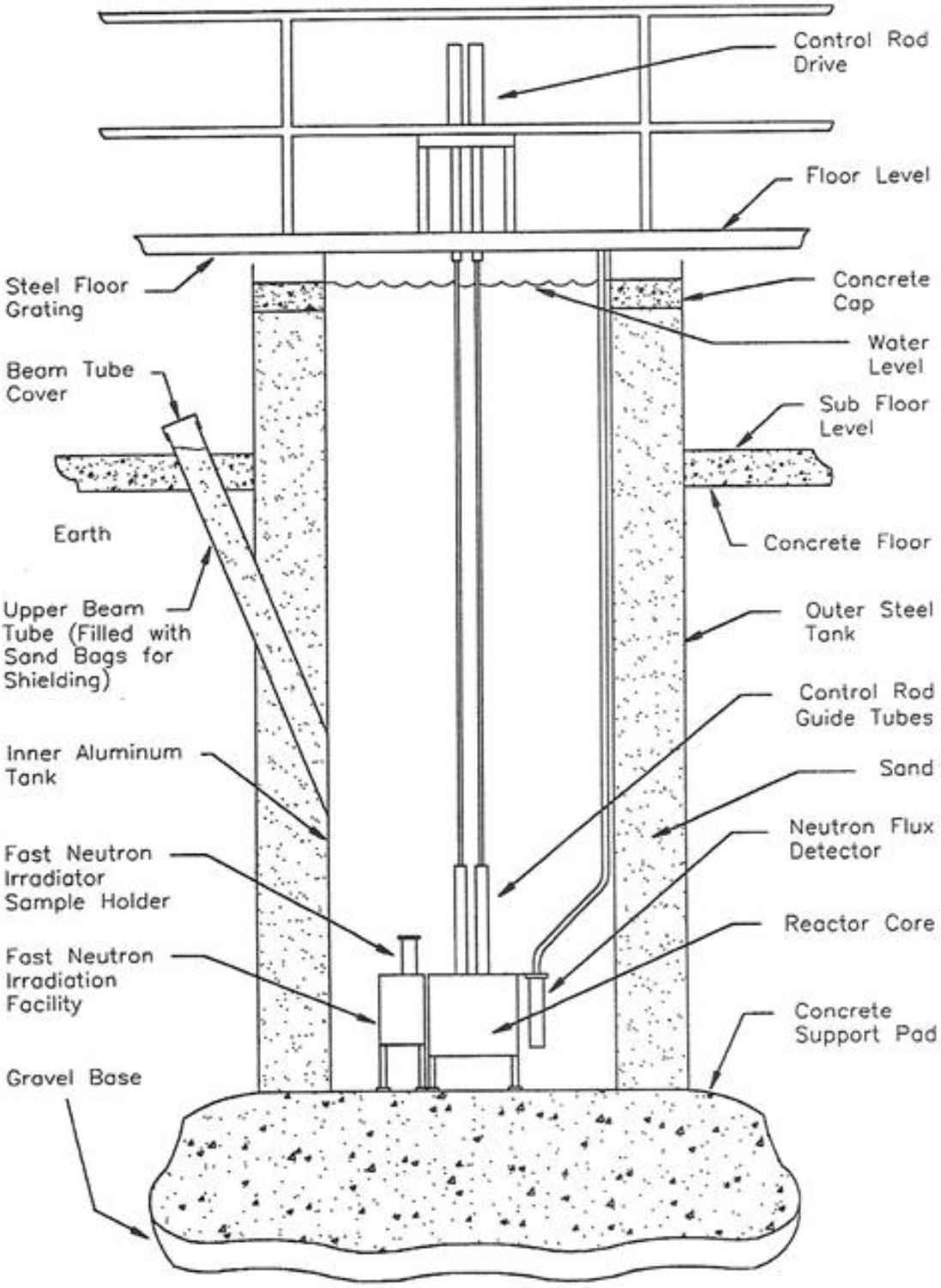

Figure 1-1. UUTR Side View [1]

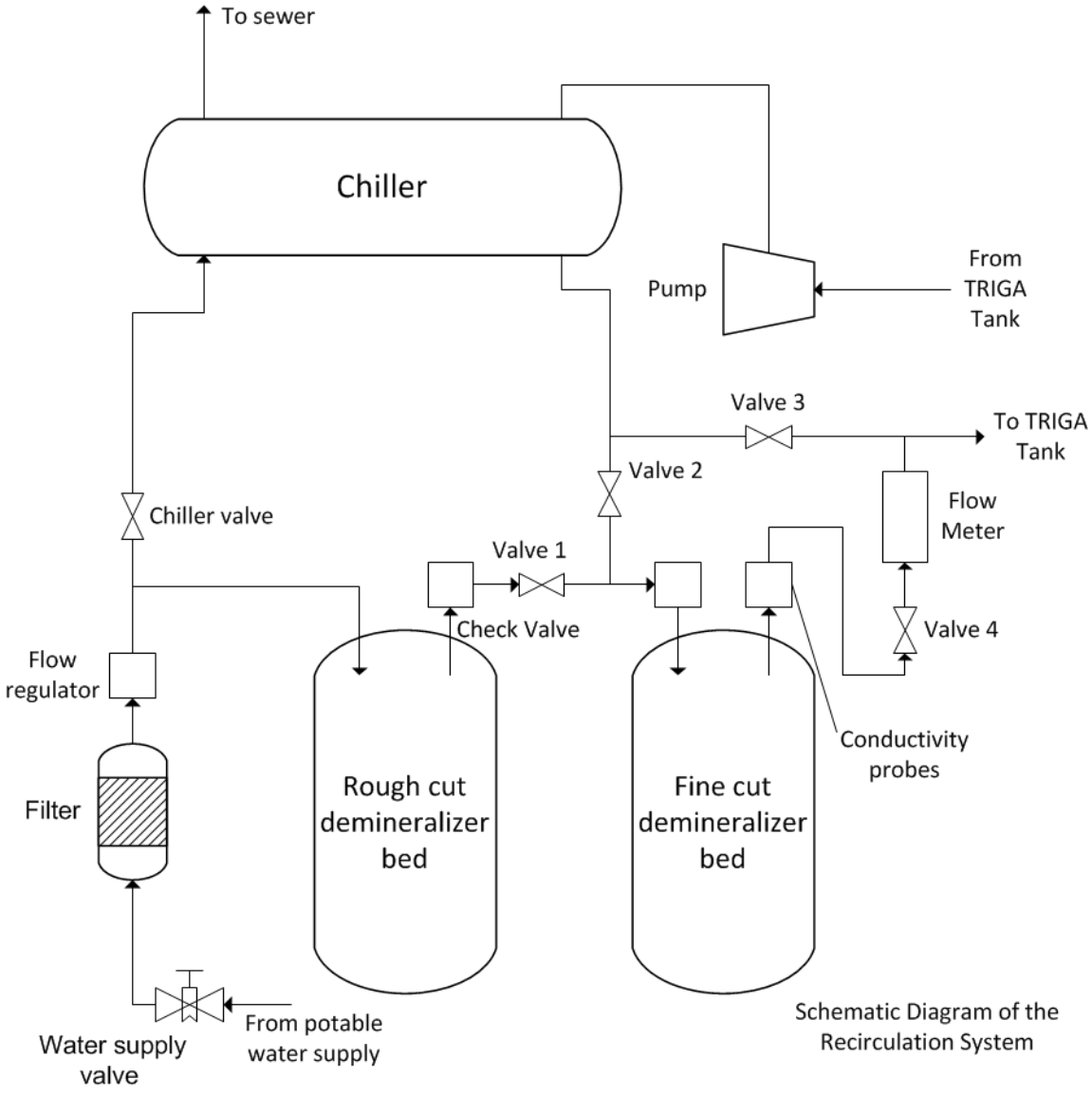

Figure 1-2. Diagram of UUTR Primary Recirculation Loop

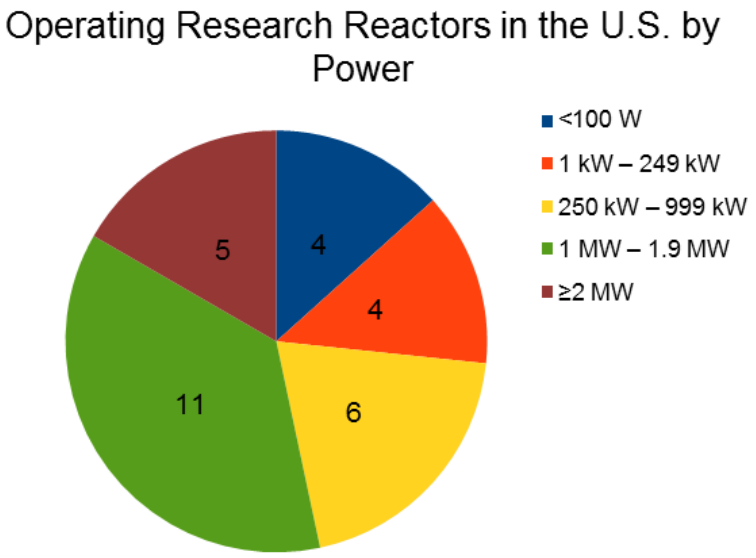

Figure 1-3. Operating Research and Test Reactors in the U.S.A. Grouped by Their Licensed Power [Data from 2]

Table 1-1. Operating Research and Test Reactors in the U.S.A. [Data from 2]

Reactor Location	City, State	Power	Cooling System
Aerotest Operations	San Ramon, CA	250 kW	yes
Armed Forces Radiobiological Research Institute	Bethesda, MD	1 MW	1.5 MW
Dow Chemical	Midland, MI	300 kW	1 MW
Idaho State University	Pocatello, ID	5 W	-
Kansas State University	Manhattan, KS	1.25 MW	1.25 MW
Massachusetts Institute of Technology	Cambridge, MA	5 MW	6 MW
National Institute of Standards and Technology	Gaithersburg, MD	20 MW	22 MW
North Carolina State University	Raleigh, NC	1 MW	yes
Ohio State University	Columbus, OH	500 kW	500 kW
Oregon State University	Corvallis, OR	1.1 MW	1 MW
Penn State University	University Park, PA	1 MW	1 MW
Purdue University	West Lafayette, IN	1 kW	no
Reed College	Portland, OR	250 kW	500 kW
Rensselaer Polytechnic Institute	Schenectady, NY	1 W (100 W max)	-
Rhode Island Atomic Energy Commission	Narragansett, RI	2 MW	2.3 MW
Texas A&M	College Station, TX	1 MW	2 MW
Texas A&M	College Station, TX	5 W	-
University of California-Davis	Davis, CA	2 MW	2 MW
University of California-Irvine	Irvine, CA	250 kW	258 kW
University of Florida	Gainesville, FL	100 kW (125 kW max)	500 kW
University of Maryland	College Park, MD	250 kW	300 kW
University of Massachusetts	Lowell, MA	1 MW	yes
University of Missouri	Columbia, MO	10 MW	yes
University of Missouri	Rolla, MO	200 kW	no
University of New Mexico	Albuquerque, NM	5 W	-
University of Texas	Austin, TX	1 MW	yes
University of Utah	Salt Lake City, UT	100 kW	25 kW
University of Wisconsin	Madison, WI	1 MW	1 MW
U.S. Geological Survey	Denver, CO	1 MW	1 MW
Washington State University	Pullman, WA	1 MW	1.3 MW

CHAPTER 2

HEAT TRANSFER PHENOMENA IN UUTR

2.1 Heat Transfer Background

As the reactor is operated energy is released through the fission process. The majority of this energy appears as energy carried by fission fragments, gamma rays, neutrons and beta particles emitted [3]. When these particles interact with the surrounding materials, heat is produced. This process heats up the fuel meat and starts the chain of heat transfer.

While there has been a great deal of research on heat transfer inside fuel and on fuel rods for TRIGA reactors [4, 5], this study focuses on the system as a whole. The fuel rods in the UUTR core heat the surrounding water which flows through the fuel channels then up and over the rods in a natural convection loop. The heated water then can either evaporate from the open top of the reactor pool or the heat is transferred to the environment. Transferring the heat to the environment can be either through the top surface which is open to the air or through the aluminum tank wall, sand barrier and outer steel tank wall. Currently, through one of these two methods is the only way the pool water is cooled back to ambient temperature.

2.2 Energy Equations

In order to determine the heat transfer into the reactor pool from the operating core, the reactor is first considered to be a closed system with a control volume surrounding the core and water. The energy equation is then:

$$E_{in} - E_{out} = \Delta E_{system} \tag{2.1}$$

where E_{in} is energy into the system (J)

E_{out} is energy out of the system (J)

ΔE_{system} is the energy balance of the system (J)

This expands to:

$$Q - W = \Delta U + \Delta KE + \Delta PE \tag{2.2}$$

As work added into the system (W), kinetic energy (KE) and potential energy (PE) are not applicable in this instance only heat transfer (Q) and internal energy (U), which has been expanded, remain the equation then becomes:

$$Q_{in} = \left(m_t C_p \Delta T\right) + m_e\left(\Delta H_V + C_p \Delta T\right) \tag{2.3}$$

where Q_{in} is heat (J)

m_t is the mass of water in the reactor tank (kg), assumed to be full at 30,000 L

C_p is the specific heat of water (4,183.2 J/kg K, at 20°C) [6]

ΔT is the temperature difference from the starting and ending conditions, in °C

m_e is mass of water evaporated (kg)

ΔH_V is latent heat of vaporization for water at 20°C (2,453.5 x10^3 J/kg) [6]

Using this equation it is possible to estimate the overall average temperature increase of the reactor tank water. From historical reactor run data included in Appendix A it was found that an average water evaporation is 2.16 kg/hr when operating at 90 kW [7]. This leads to a temperature increase per hour of 2.58°C. Table 2-1 shows calculated values for higher theoretical UUTR power levels.

Because these power levels are theoretical values, they do not include the evaporative portion of the equation. This amount is variable and dependent on current atmospheric and starting conditions, but judging from the prior data in Appendix A it would lower the temperatures in Table 2-1 by 2-4% with a greater amount of water being evaporated [7].

2.3 Energy Lost through Conduction

In addition to the system losing energy through evaporation it is also lost through conduction. The heat generated in the fuel is transferred to the water through natural convection, from the water to the aluminum, sand and steel enclosures by conduction and is finally cooled by the ambient air through convection. To gain a complete understanding of the heat loss from UUTR it was necessary to investigate the conduction process and gauge its significance.

For modeling the heat flow from the core to the outside surface a cylindrical thermal circuit of the system was created following the conventions set forth by [8]. First, Fourier's law of heat transfer is expressed in cylindrical form:

$$q_r = -k(2\pi rL)\frac{dT}{dr} \tag{2.4}$$

where q_r is heat rate (W)

k is thermal conductivity (W/m-K)

r is radial distance (m)

L is cylindrical length (m)

T is temperature (K)

Applying the general solution to this equation and using the temperatures of the inner and outer surface as boundary conditions creates an expression for the heat transfer rate.

$$q_r = \frac{2\pi Lk(T_{S,1}-T_{S,2})}{\ln\frac{r_2}{r_1}} \tag{2.5}$$

When using the thermal circuit model the material properties and dimensions are separated out of Eq (2.5) to calculate the total thermal resistance. Eq (2.6) is the cylindrical thermal resistance for conduction:

$$R_{cond} = \frac{\ln\frac{r_2}{r_1}}{2\pi Lk} \tag{2.6}$$

while for convection the following relation is applied:

$$R_{conv} = \frac{1}{2\pi r_1 Lh_1} \tag{2.7}$$

where R is thermal resistance (K/W)

h is heat transfer coefficient (W/m^2-K)

The insulating materials in UUTR are arrayed in a serial configuration so the thermal circuit takes the form as shown in Figure 2-1 and with Eq (2.8). In this form the heat transfer to the outside surface of the steel tank is given by knowing the temperature of the core (in contact with the water) and temperature of the outer stainless steel tank.

$$q_r = \frac{(T_{core} - T_{SS,2})}{\left(\frac{1}{2\pi r_{core} L_{core} h}\right) + \left(\frac{\ln \frac{r_{Al,2}}{r_{Al,1}}}{2\pi k_{Al} L_{Al}}\right) + \left(\frac{\ln \frac{r_{sand,2}}{r_{sand,1}}}{2\pi k_{sand} L_{sand}}\right) + \left(\frac{\ln \frac{r_{SS,2}}{r_{SS,1}}}{2\pi k_{SS} L_{SS}}\right)} \tag{2.8}$$

2.4 Calculation of the Heat Transfer Coefficient

In order to use Eq (2.8) and find the energy loss though the tank walls the convective heat transfer coefficient (h) of the tank water must first be calculated. The first step in this process is the calculation of the dimensionless Grashof number, representing a measure of the ratio of the buoyancy forces to the viscous forces acting on the fluid [8].

$$Gr = \frac{g\beta(T_{core} - T_{water})L_{core}^3}{\nu^2} \tag{2.9}$$

where Gr is Grashof number

g is gravitational acceleration (m/s^2)

β is volumetric thermal expansion coefficient of water (207.71 x10^{-6} K^{-1}, at 20°C) [8]

T is temperature (K)

L is length (m)

v is kinematic viscosity of water (1.0058 x10^{-6} m^2/s, at 20°C) [8]

This result is multiplied by the Prandtl number for water at 20°C to give the Rayleigh number, a measure of the magnitude of buoyancy and viscous forces in the water.

It was decided to use the heated, upward-facing, flat plate correlation to model the reactor core. This correlation calculates the ratio of conductive to convective heat transfer known as the Nusselt number (Nu). Based on the calculated Rayleigh number and the chosen correlation the following relation is used [8]:

$$Nu = 0.15Ra^{1/3} \tag{2.10}$$

After finding the Nusselt number the heat transfer coefficient (h) can be known through their relationship derived from Newton's law of cooling.

$$Nu = \frac{hL}{k} \tag{2.11}$$

where L is the heated length (m)

k is thermal conductivity (W/m-K)

Figure 2-2 summarizes this process and shows the results of each step. After this value is known the calculation can proceed to obtain the overall thermal resistance of the reactor system using Eq (2.8).

2.5 Calculation of Conduction Heat Loss

The heat transfer coefficient for the reactor tank water, calculated in Section 2.4 to be 704.84 W/m^{2}K, was inserted into Eq (2.8) with the remaining variables defined in Table 2-2 to calculate the heat lost through conduction. The total thermal resistance (R) calculated for UUTR was 0.019 K/W. This results in a loss of 1,590 W of heat through conduction to the outer wall while operating at 90 kW.

2.6 Discussion

When UUTR is at 90 kW, it was found that the typical range for evaporative energy was 1.8-3.6 kW while only 1.59 kW were transferred through conduction. These methods only account for a maximum 5.77% of the total power generated. The remaining continues to heat the tank water through natural convection until it is eventually removed passively to the environment or actively by a heat exchanger. In Chapters 3 and 4 the simulations of this heating process in greater detail are described; the cooling systems are then discussed in Chapter 7.

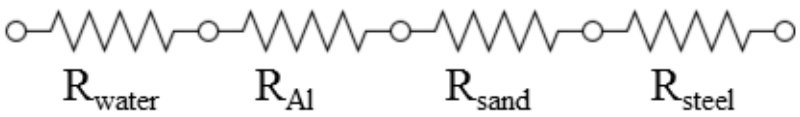

Figure 2-1. Thermal Circuit Diagram for UUTR

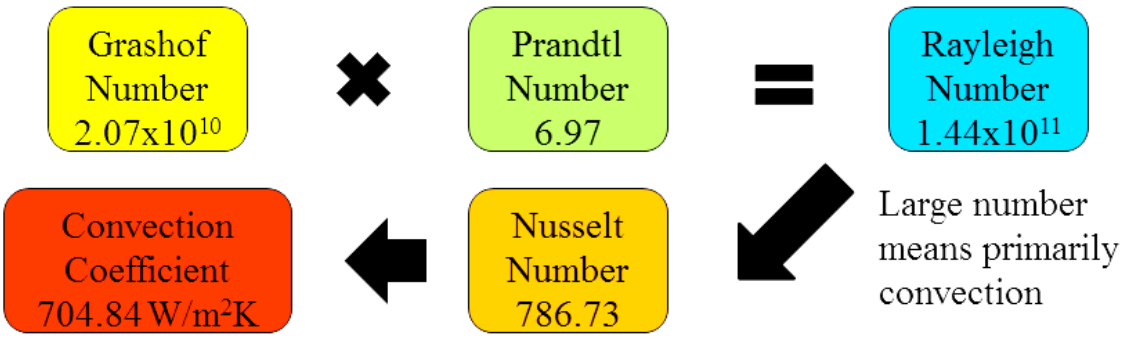

Figure 2-2. Process of Determining the Convection Heat Transfer Coefficient

Table 2-1. Temperature Increases per Hour for Higher UUTR Power Levels

Power Level (kW)	Temperature Rise/Hour (°C)
100	2.87
200	5.74
300	8.60
400	11.47
500	14.34

Table 2-2. Variables Affecting UUTR Heat Conduction

Variable	Description	Value (Units)
T_{core}	Fuel temperature contacting water at 90 kW	53.7 (°C) [1]
$T_{SS,2}$	Temperature of outer SS wall	23.0 (°C)
r_{core}	Core radius	0.29 (m)
L_{core}	Core height	0.67 (m)
h	Heat transfer coefficient of water	704.84 (W/m^2-K)
$r_{Al,1}$	Inner radius of Al tank	1.17 (m)
$r_{Al,2}$	Outer radius of Al tank	1.18 (m)
k_{Al}	Thermal conductivity of Al	177 (W/m-K) [6]
L_{Al}	Height of Al tank	7.32 (m)
$r_{sand,1}$	Inner radius of sand layer	1.18 (m)
$r_{sand,2}$	Outer radius of sand layer	1.48 (m)
k_{sand}	Thermal conductivity of sand	0.27 (W/m-K) [6]
L_{sand}	Height of sand layer	7.32 (m)
$r_{SS,1}$	Inner radius of SS tank	1.48 (m)
$r_{SS,2}$	Outer radius of SS tank	1.485 (m)
k_{SS}	Thermal conductivity of SS	14.9 (W/m-K) [6]
L_{SS}	Height of SS tank	7.32 (m)

CHAPTER 3

SOLIDWORKS BASED ASESSMENT OF UUTR HEAT TRANSFER AND THERMAL-HYDRAULICS PHENOMENA

3.1 Introduction

The SolidWorks design software and Flow Simulation package [9] were used to model the overall setup of the UUTR tank to visualize and quantify the natural convective cooling process of the core, especially over longer operation. These results were compared to temperature measurements taken during reactor operations to help validate the model. The same model is then used to assess the conditions at higher core power levels.

3.2 SolidWorks and SolidWorks Flow Simulation

SolidWorks is a 3-D computer-aided-design (CAD) software suite currently developed by Dassault. It allows creation and manipulation of 3-D parts and assemblies using a parametric design approach. SolidWorks is widely used in engineering fields for product design, testing and manufacture [10].

SolidWorks Flow Simulation is a fluid dynamics and thermal simulation program that works through SolidWorks models and assemblies. The software works using the finite volume (FV) solution method to solve the governing

equations over the computational mesh. Because the equations are discretized over each volume, values for each surface can be known making this method conservative [11].

The governing equations are the time-averaged Navier-Stokes equations for conservation of mass (3.1), momentum (3.2) and energy (3.3) in a fluid system.

$$\frac{\partial \rho}{\partial t} + \frac{\partial}{\partial x_i}(\rho u_i) = 0 \tag{3.1}$$

$$\frac{\partial \rho u_i}{\partial t} + \frac{\partial}{\partial x_j}\left(\rho u_i u_j\right) + \frac{\partial p}{\partial x_i} = \frac{\partial}{\partial x_j}\left(\tau_{ij} + \tau_{ij}^R\right) + S_i \quad i = 1,2,3 \tag{3.2}$$

$$\frac{\partial \rho H}{\partial t} + \frac{\partial \rho u_i H}{\partial x_i} = \frac{\partial}{\partial x_i}\left(u_j\left(\tau_{ij} + \tau_{ij}^R\right) + q_i\right) + \frac{\partial p}{\partial t} - \tau_{ij}^R \frac{\partial u_i}{\partial x_j} + \rho\varepsilon + S_i u_i + Q_H \tag{3.3}$$

where u is fluid velocity (m/s)

ρ is fluid density (kg/m^3)

$S_i = -\rho g_i$ is the external force per unit mass from buoyancy along direction I (N)

h is thermal enthalpy (J/kg)

Q_H is heat source per unit volume (W/m^3)

τ_{ik} is viscous shear stress (Pa)

τ^R is Reynolds shear stress = $\mu_t\left(\frac{\partial u_i}{\partial x_j} + \frac{\partial u_j}{\partial x_i} - \frac{2}{3}\delta_{ij}\frac{\partial u_k}{\partial x_k}\right) - \frac{2}{3}\rho k \delta_{ij}$ (Pa)

q_i is diffusive heat flux (W)

$H = h + u^2/2$

When needed the above equations can be supplemented by additional equations to define changes in the state of the fluid, viscosity or the thermal conductivity

through materials. In this case only thermal conductivity is needed and is represented as follows:

$$q_i = \left(\frac{\mu}{Pr} + \frac{\mu_t}{\sigma_c}\right)\frac{\partial h}{\partial x_i} \tag{3.3}$$

$$\frac{\partial \rho e}{\partial t} = \frac{\partial}{\partial x_i}\left(\lambda_i \frac{\partial T}{\partial x_i}\right) + Q_H \tag{3.4}$$

where μ is dynamic viscosity and turbulent eddy viscosity (Pa-s)

k is turbulent kinetic energy (J)

h is thermal enthalpy (J/kg)

Pr is Prandtl number

σ_c is constant, 0.9

q_i is heat flux (W)

e is specific internal energy (J/kg)

λi is thermal conductivity eigenvalues

Q_H is released heat per volume (J/m^3)

This setup allows for treatment of both laminar and turbulent flow. For turbulent cases kinetic energy dissipation is dealt with using the k-ε model [11, 12].

3.3 Creation of the Simulation Model

The basic elements of the UUTR were modeled including the tank, walls, core and water and all were placed in a SolidWorks assembly file. Dimensions and materials were kept the same as those referenced in Section 1.1. A view of the

geometry as built in SolidWorks is shown in Figure 3-1 (walls have been made transparent for ease of viewing).

Creating the model in this simple fashion allowed for more reasonable computation times while still achieving the goals of temperature measurement and flow visualization. In the Flow Simulation software the computational domain was applied up to the outer wall edge and a 3-D rectangular mesh was selected. Using mesh refinement a minimum gap size of 0.79 inches (0.02 meters) was specified. It was found that this size resulted in complete and small enough coverage without greatly increasing computation times. Images of the created mesh are shown in Figure 3-2 and the mesh statistics are shown in Table 3-1. The mesh near the walls and core has a finer resolution for better modeling of the thermal and velocity boundary layers whereas in the center of the tank the mesh is coarse.

3.4 Flow Simulation Setup

The analysis was carried out using an internal simulation with time dependency and gravity enabled (-9.81 m/s in the y direction). Water was chosen as the working fluid to fill the tank. The variable properties of density, dynamic viscosity, specific heat (C_p) and thermal conductivity are defined in Table 3-2 over the range of 20° – 70°C with the software using a linear interpolation for intermediate values. Starting temperature for the simulations was set at 20°C or 24°C and air pressure at 1 atm.

The interior walls of the aluminum tank were defined to act as a real wall with the heat transfer coefficient set as -704.84 W/m^2-K (negative sign convention, reference Figure 2-2). The core was defined as a surface heat source with a constant, overall heat flux equal to the reactor's power level. Simulation time was

set to run for a total of 6 hours (21,600 sec) with results being recorded at each hour. Global goals were setup in the program to track the fluid temperature and velocity over the course of the simulation. A complete list of input data for the simulations is included in Appendix B. The simulations were run on the College of Engineering's server, a dual-processor, 64-bit AMD Opteron, dual-core system with 32 GB of RAM and running Windows Server 2008.

3.5 Results

Power levels from 90 to 250 kW were simulated in 10 kW increments for a 6 hour run time. Each was started from an initial temperature of 20°C. Additionally, a single 90 kW, 1 hour simulation was run with a starting temperature of 24°C. Temperature measurements were taken at an arbitrary location 4.5 meters (14.76 feet) from the base of the reactor tank along the center axis. This location was chosen as it proved to be an area of even temperature distribution to represent the overall heating of the reactor tank water. The results from the 20°C simulation are shown plotted in Figure 3-3 and presented in full in Table 3-3.

Additionally, as a visual aid temperature contour and velocity plots were created to better compare the 20°C 90 and 250 kW simulations. These are shown in Figures 3-4 and 3-5. Both temperature contour plots show the more uniform temperature distribution that is present in the SolidWorks simulations that leads to more accurate temperature results. The velocity plots both show examples of vortex shedding caused by fluid movement over the core surface with the 250 kW core having a more pronounced effect from the higher fluid velocities in the convection column.

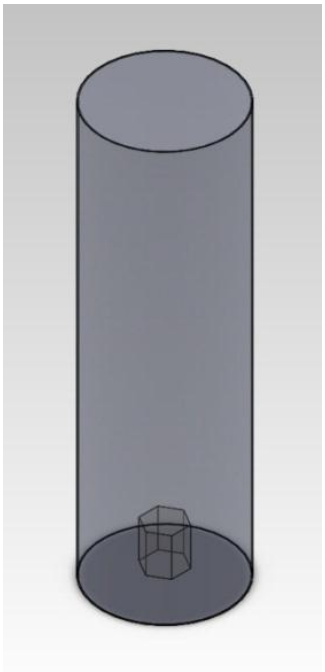

Figure 3-1. SolidWorks Model of the UUTR

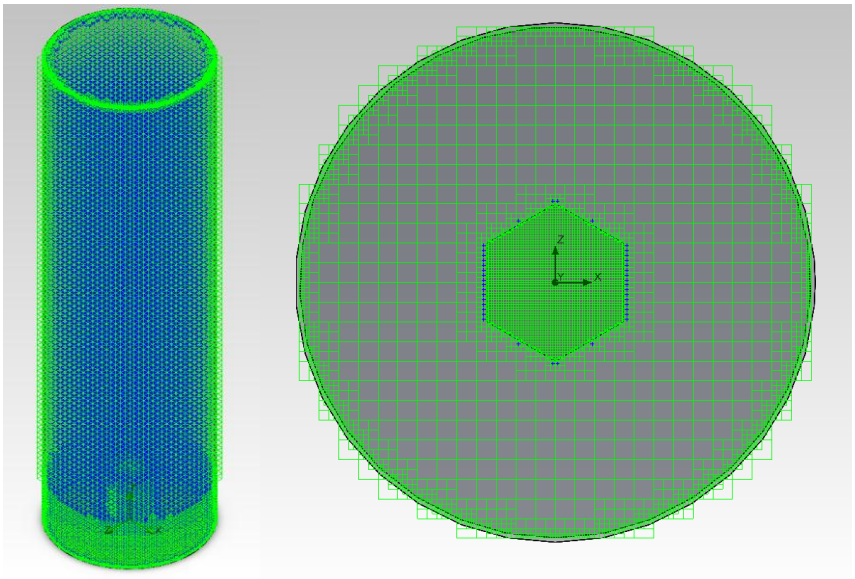

Figure 3-2. Isometric and Bottom Views of Flow Simulation Mesh

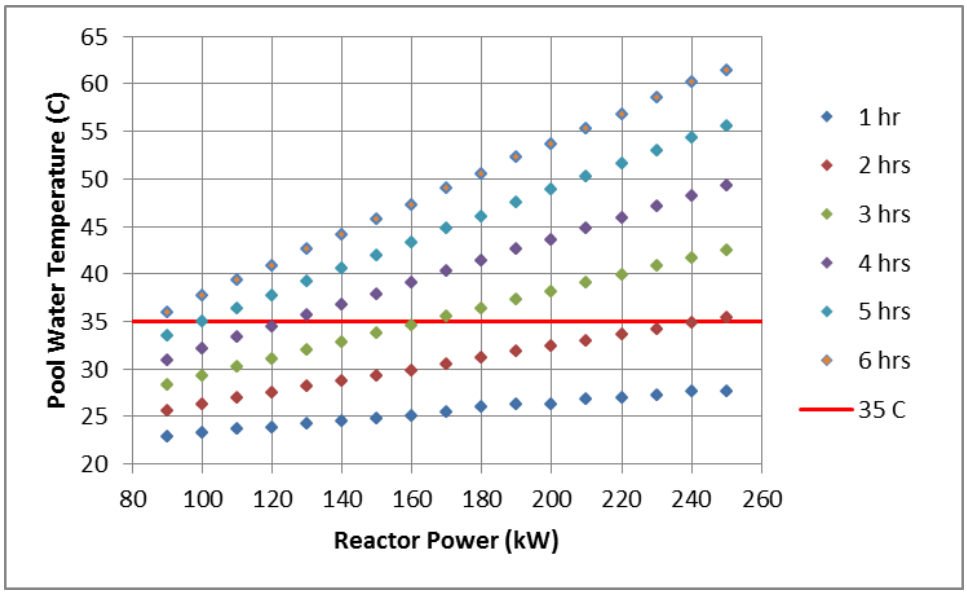

Figure 3-3. UUTR Pool Water Temperature as a Function of UUTR Power as Obtained with SolidWorks Flow Simulation

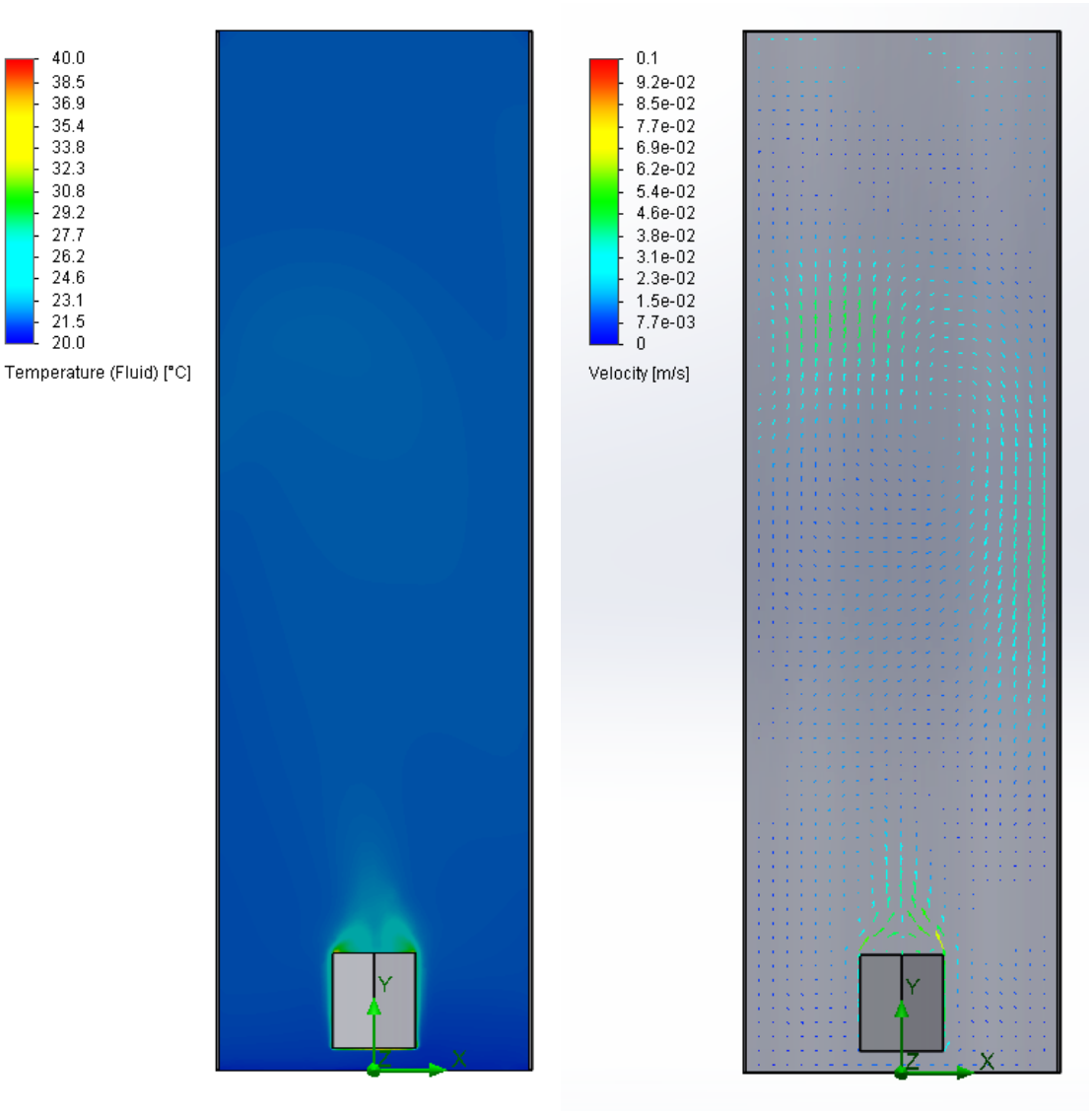

Figure 3-4. Temperature and Velocity Contours at 90 kW after 1 Hour Runtime

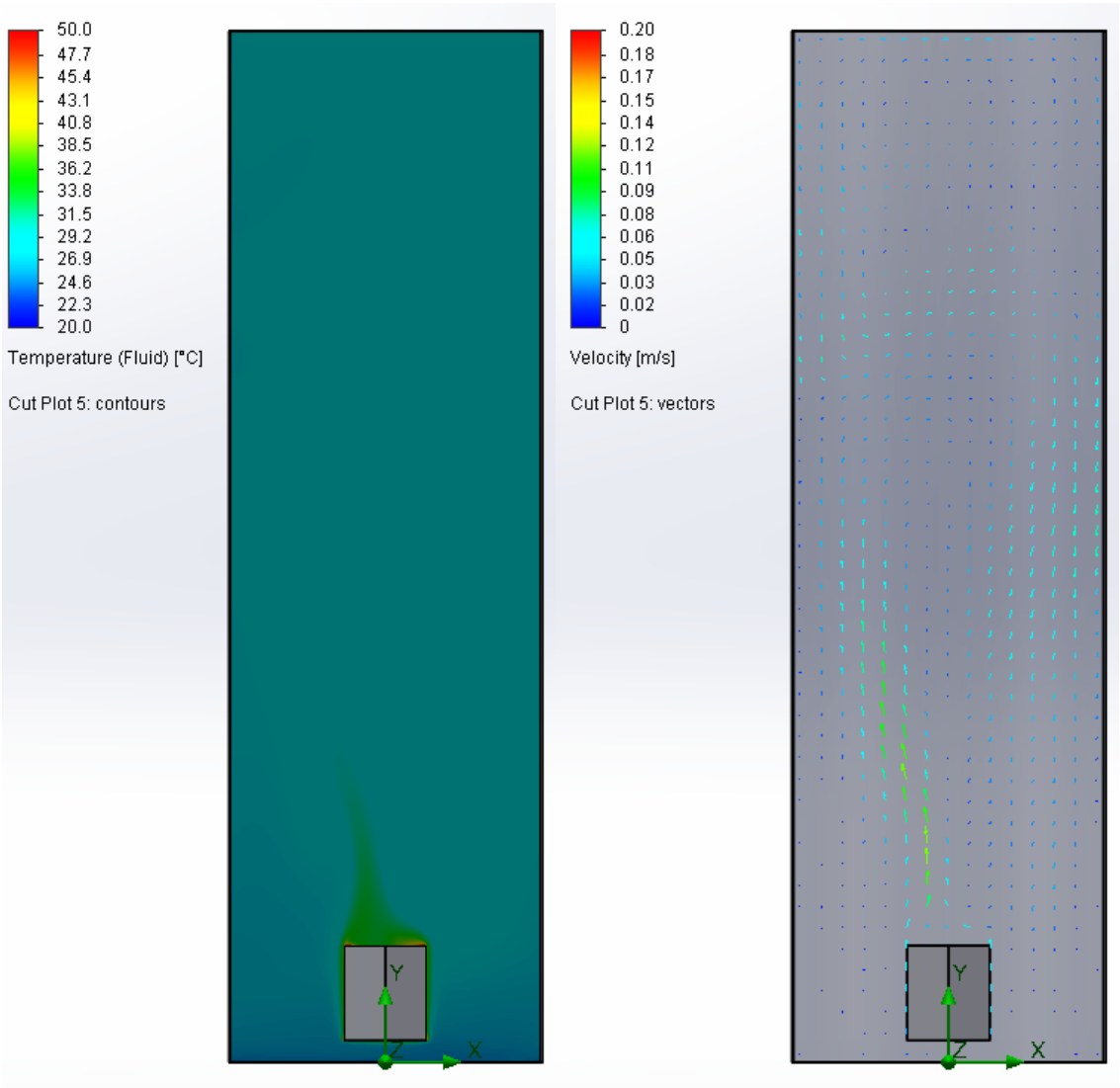

Figure 3-5. Temperature and Velocity Contours at 250 kW after 1 Hour Runtime

Table 3-1. Flow Simulation Mesh Statistics

Cell Type	Number
Fluid Cells	70,800
Solid Cells	17,080
Partial Cells	27,840
Total	115,720

Table 3-2. Variable Properties of Water

Temperature (°C)	Density (kg/m^3)	Dynamic Viscosity (Pa-s)	Specific Heat (J/kg-K)	Thermal Conductivity (W/m-K)
20	998.16	1.0014×10^{-3}	4,184.4	0.59843
25	997.00	8.8990×10^{-4}	4,181.6	0.60717
30	995.60	7.9719×10^{-4}	4,180.1	0.61547
35	993.99	7.1917×10^{-4}	4,179.5	0.62330
40	992.17	6.5285×10^{-4}	4,179.6	0.63060
45	990.17	5.9595×10^{-4}	4,180.4	0.63736
50	987.99	5.4674×10^{-4}	4,181.6	0.64356
55	985.65	5.0388×10^{-4}	4,183.2	0.64923
60	983.16	4.6631×10^{-4}	4,185.1	0.65436
65	980.15	4.3318×10^{-4}	4,187.5	0.65897
70	977.73	4.0382×10^{-4}	4,190.2	0.66310

Table 3-3. Six Hour Runtime Simulation Results as Obtained with SolidWorks Flow Simulation

Reactor Power (kW)	Temp at 1 hr (°C)	Temp at 2 hrs (°C)	Temp at 3 hrs (°C)	Temp at 4 hrs (°C)	Temp at 5 hrs (°C)	Temp at 6 hrs (°C)
90	22.86	25.61	28.36	30.95	33.46	35.93
100	23.35	26.34	29.29	32.20	34.99	37.69
110	23.72	26.90	30.19	33.37	36.42	39.33
120	23.85	27.45	31.02	34.40	37.69	40.83
130	24.28	28.15	32.03	35.69	39.24	42.61
140	24.48	28.69	32.83	36.74	40.59	44.17
150	24.75	29.34	33.76	37.91	41.94	45.78
160	25.05	29.87	34.60	39.03	43.30	47.30
170	25.42	30.55	35.51	40.26	44.76	49.02
180	25.97	31.16	36.38	41.39	46.09	50.51
190	26.29	31.82	37.34	42.59	47.57	52.28
200	26.34	32.36	38.17	43.62	48.83	53.67
210	26.81	33.01	39.10	44.83	50.25	55.32
220	26.96	33.57	39.96	45.91	51.58	56.72
230	27.23	34.16	40.81	47.08	53.03	58.50
240	27.66	34.82	41.70	48.21	54.35	60.15
250	27.71	35.36	42.52	49.23	55.49	61.39

CHAPTER 4

FLUENT MODEL OF THE UUTR

4.1 Introduction

The Fluent simulation package from Ansys [13] was used to create a more detailed model of the UUTR core. This model simulated the UUTR tank convection processes over higher power levels but a shorter time frame. The model was also validated with temperature measurements taken during normal operations.

4.2 Ansys Fluent

Fluent is a computational fluid dynamics (CFD) code currently developed by Ansys. The code supports 2-D or 3-D model meshes and provides comprehensive simulation capabilities for a wide range of incompressible and compressible, laminar and turbulent fluid flow problems. Simulations can be steady-state or transient and also includes the ability to model various forms of heat transfer such as conjugate, radiation and convection [14]. Fluent is commonly used in product design and optimization and as a tool in thermodynamics and fluidics research. For this analysis Fluent was used inside the commercially packaged Ansys Workbench platform.

The software is based on the finite element method (FEM). A computational mesh is generated for the model being analyzed with the defining equations

applied over each mesh element. Boundary conditions are defined at all mesh edges (walls) creating a conservative system where individual element values can be known [14].

For all simulations Fluent solves the continuity equations of mass (4.1) and momentum (4.2). If heat transfer is involved the energy equation (4.3) is also added [14].

$$\frac{\partial \rho}{\partial t} + \nabla \cdot (\rho \vec{v}) = S_m \tag{4.1}$$

$$\frac{\partial}{\partial t}(\rho \vec{v}) + \nabla \cdot (\rho \vec{v} \vec{v}) = -\nabla p + \nabla \cdot (\overline{\tau}) + \rho \vec{g} + \vec{F} \tag{4.2}$$

$$\frac{\partial}{\partial t}(\rho E) + \nabla \cdot \left(\vec{v}(\rho E + p)\right) = \nabla \cdot \left(k_{eff} \nabla T - \sum_j h_j \vec{J}_j + \left(\overline{\tau}_{eff} \cdot \vec{v}\right)\right) + S_h \tag{4.3}$$

where ρ is fluid density (kg/m3)

t is time (s)

v is velocity vector (m/s)

S_m is mass added from any sources (kg)

p is static pressure (Pa)

g is gravitational vector (m/s^2)

F is external body forces (N)

τ is stress tensor = $\mu\left((\nabla \vec{v} + \vec{v}^T) - \frac{2}{3}\nabla \cdot \vec{v} I\right)$ (Pa)

μ is molecular viscosity (Pa-s)

I is unit tensor

k_{eff} is effective conductivity (S/m)

J is the diffusion flux of j (kg/m^2-s)

S_h is energy from external or volumetric heat sources (J)

$E = h - \frac{p}{\rho} + \frac{v^2}{2}$

h is enthalpy (J/kg)

As with the Flow Simulation software, Fluent can model many other fluid and thermodynamic conditions as the user activates add-on equations.

4.3 Creation of the Fluent Model

The tank, walls, core and water of UUTR were modeled to their original dimensions (as reported in Section 1.1) in the DesignModeler program included with the Ansys simulation package. During this process the UUTR core was further discretized into zones so that the pin power distribution could be mapped to the surface. The 3-D model is shown in Figure 4.1.

In the Ansys meshing program the created geometry was opened and a tetrahedral shaped mesh and CFD physics preference were chosen. A coarse relevance center was used with medium smoothing and a slow transition area around the core for increased flow detail in that region. The generated mesh is shown in Figure 4-2 and its statistics are presented in Table 4.1. After the mesh was created all of the wall faces and discretized core sections were named to facilitate their recognition by Fluent. The mesh was then loaded into the Fluent solver.

4.4 Fluent Simulation

In the Fluent software the imported mesh is checked for connectivity and correct volume. Then the solver is set to perform a pressure-based, absolute, transient simulation with gravity enabled (-9.81 m/s^2 in the *y* direction). For this simulation the energy equation is enabled and the laminar model is used. In the materials section the fluid is set to liquid water and the solid materials are defined to be aluminum. The properties specified for each of these materials (at 20°C) are shown in Table 4-2. Also, water density was defined to follow a Boussinesq approximation. The Boussinesq model for natural convection flows gives faster convergence than having the fluid density as a function of temperature. The model assumes fluid density is constant in all solved equations except in the momentum Eq (4.2) where it is replaced by Eq (4.4). The approximation is accurate as long as $\beta(T-T_0)<<1$ which applies for all cases during these simulations [15].

$$\rho = \rho_0(1 - \beta\Delta T) \tag{4.4}$$

where ρ is new density (kg/m^3)

ρ_0 is constant density (kg/m^3)

β is thermal expansion coefficient of water (207 x10^{-6} K^{-1})

The next step involves defining the cell zones and boundary conditions. Under the Cell Zone Conditions section the interior zone is changed to a fluid and edited to contain the water defined in the above steps. In the Boundary Conditions section all named wall sections created in the meshing process appear. The side and bottom tank walls are defined as convection/conduction boundaries between

the water and aluminum while the top is defined as a convection boundary open to the atmosphere. Both use the heat transfer coefficient defined in Ch. 2 and specify a room temperature of 22°C. The core surfaces are defined as thermal boundaries with a heat flux. Following the same practice as in the Safety Analysis Report (SAR) [1], the core was discretized into sixths for entry into the software as shown in Figure 4-3 to facilitate the power mapping onto the thermal boundaries in the model.

To increase simulation speed and aid in modeling, the top and bottom surfaces were divided into ring sections corresponding to the fuel element rings to aid in mapping the power distribution to the thermal boundaries. The pin power distributions [1, 16] and core surface area were used to determine the heat flux as follows:

$$\frac{Power\ Distribution\ [kW]}{Surface\ Area\ [m^2]} = Heat\ Flux\ [\frac{kW}{m^2}] \tag{4.5}$$

The process of dividing the core up into sections and then using the pin power distributions to calculate the heat flux for each thermal boundary was repeated for each power lever that was simulated. The heat flux values varied based on the total reactor power and core layout.

Analysis was carried out using the Pressure Implicit with Splitting of Operators (PISO) solution algorithm with the spatial discretization of pressure set to second order, the recommended settings for buoyancy driven flows. This solution method assumes a higher degree of relation between the corrections for pressure and velocity and can greatly reduce the number of iterations required for

convergence, especially in transient cases [14]. The remainder of the solution settings were left at the default values and are listed in their entirety in Appendix C. Under-relaxation factors for the solution controls were also left at the default values. The solution was initialized to start at a temperature of either 20°C (293°K) or 24°C (297°K) and calculation activities were set up to record fluid temperature and velocity at 5 minute intervals. After this setup the solver was run with a 1 second time step until a maximum simulation time of 3,600 seconds was reached. All simulations were run on the College of Engineering's server, a dual-processor, 64-bit AMD Opteron, dual-core system with 32 GB of RAM and running Windows Server 2008.

4.5 Fluent Results

Power levels of 90, 100, 150, 300, 400 and 500 kW were simulated for a 1 hour run time. Each was started from an initial temperature of 20°C (293°K). A 90 kW, 1 hour run time simulation was also run with a starting temperature of 24°C (297°K). Temperatures were taken at the same 4.5 meter (14.76 foot) distance from the bottom of the reactor pool and at predetermined radial distances. The results from the 20°C initial temperature simulation are presented in Table 4-3.

Fluent visualizations have also been generated for each UUTR power level. They provide a snapshot of the dynamic fluid flow at taken at 1 hour. A vertical temperature contour plot through the center-right plane, a horizontal temperature contour plot through the 4.5 meter plane and a vertical velocity vector diagram through the center-right plane are described for every simulated UUTR power level in the following sections.

4.5.1. Fluent 1 Hour Temperature and Velocity for the 90 kW Core

Figure 4.4 is the temperature contour plot from the center-right, vertical plane showing the 90 kW core's convection current as it rises over the height of the reactor pool. Figure 4.5 is the temperature contour plot from the 4.5 meter, horizontal plane showing the distribution of the convection current at 4.5 meters above the pool's base. Figure 4.6 is the velocity vector plot from the center-right, vertical plane showing the water velocity in the rising convection current of the 90 kW core.

4.5.2. Fluent 1 Hour Temperature and Velocity for the 100 kW Core

The temperature contour plot at the center-right, vertical plane showing the 100 kW core's convection current as it rises over the height of the reactor pool is shown in Figure 4.7. Figure 4.8 depicts the temperature contour plot at the 4.5 meter, horizontal plane showing the distribution of the convection current at 4.5 meters above the pool's base. Figure 4.9 shows the velocity vector plot from the center-right, vertical plane showing the water velocity in the rising convection current of the 100 kW core.

4.5.3. Fluent 1 Hour Temperature and Velocity for the 150 kW Core

Figure 4.10 is the temperature contour plot at the center-right, vertical plane showing the 150 kW core's convection current as it rises over the height of the reactor pool. Figure 4.11 shows the temperature contour plot at the 4.5 meter, horizontal plane showing the distribution of the convection current at 4.5 meters above the pool's base. Figure 4.12 shows the velocity vector from the center-right,

vertical plane showing the water velocity in the rising convection current of the 150 kW core.

4.5.4. Fluent 1 Hour Temperature and Velocity for the 300 kW Core

The temperature contour plot at the center-right, vertical plane showing the 300 kW core's convection current as it rises over the height of the reactor pool is shown in Figure 4.13, while Figure 4.14 shows the temperature contour plot at the 4.5 meter height horizontal plane. Figure 4.15 depicts the velocity vector plot from the center-right, vertical plane showing the water velocity in the rising convection current of the 300 kW core.

4.5.5. Fluent 1 Hour Temperature and Velocity for the 400 kW Core

Figure 4.16 captures the temperature contours at the center-right, vertical plane of the 400 kW core's convection current moving up the height of the reactor pool and Figure 4.17 shows the temperature contour plot at the 4.5 meter horizontal plane. Figure 4.18 is the velocity vector plot from the center-right, vertical plane of the water velocity in the convection current of the 400 kW core.

4.5.6. Fluent 1 Hour Temperature and Velocity for the 500 kW Core

Figure 4.19 shows the temperature contour plot at the center-right, vertical plane of the 500 kW core's convection current and Figure 4.20 shows the temperature contour plot at the 4.5 meter height horizontal plane. Figure 4.21 depicts the velocity vector plot from the center-right, vertical plane showing the water velocity in the convection current of the 500 kW core.

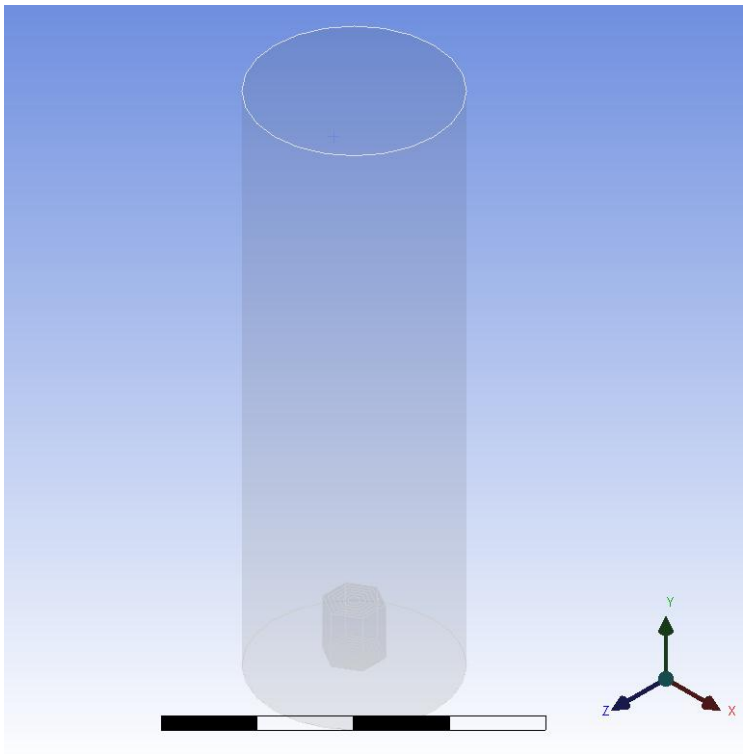

Figure 4-1. UUTR Model in Fluent

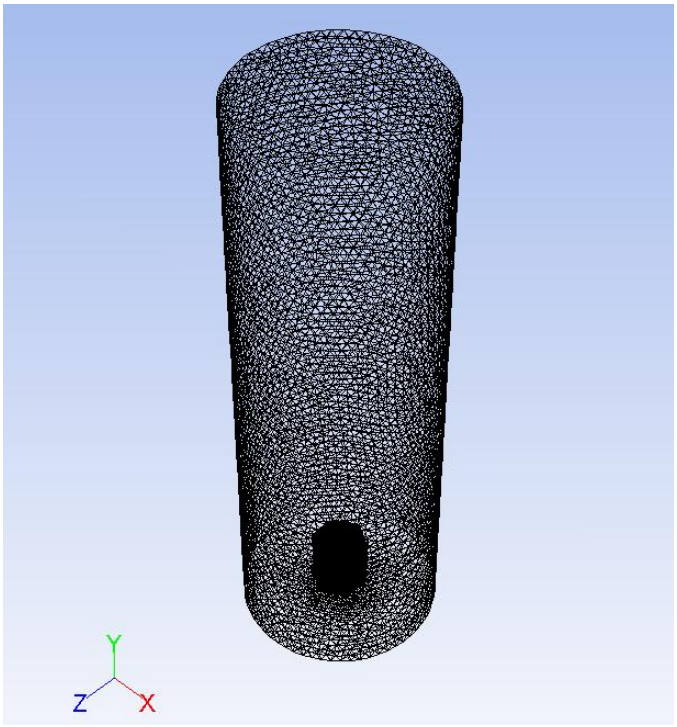

Figure 4-2. External Surfaces of Fluent Mesh

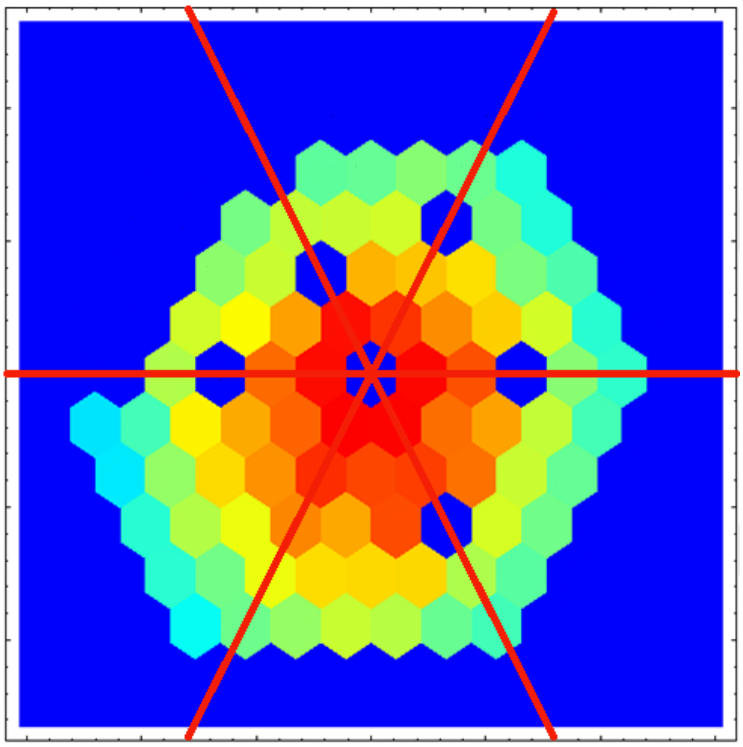

Figure 4-3. Discretizing the Core Sides Prior to Simulation (90 kW Core) [1]

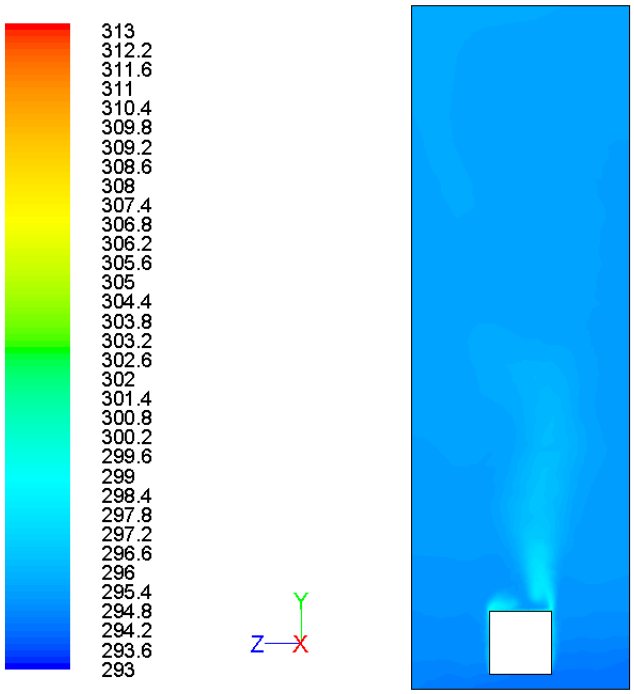

Figure 4-4. Temperature Contour Plot of 90 kW Simulation after 1 Hour Runtime

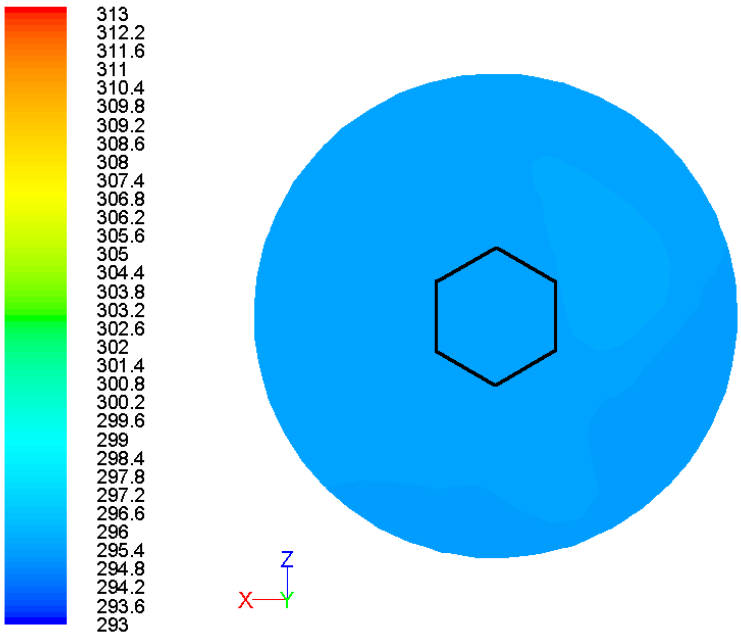

Figure 4-5. Temperature Contour Plot of 90 kW Simulation after 1 Hour Runtime, 4.5 meter Plane

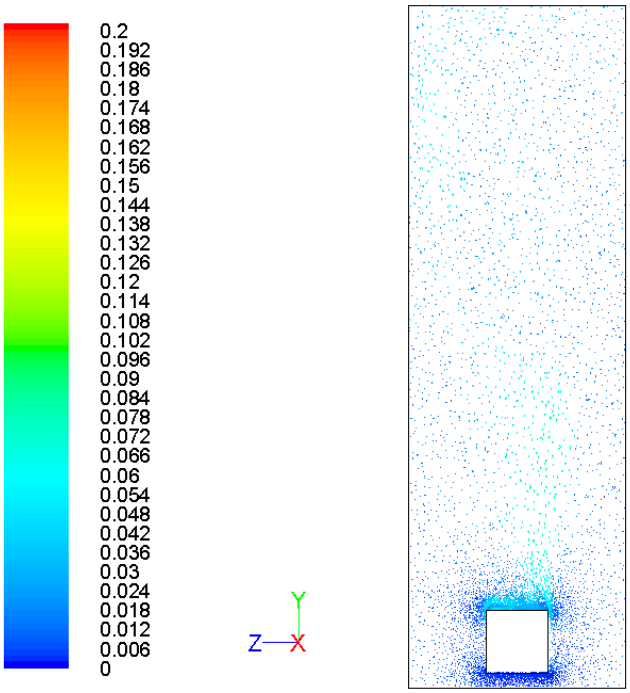

Figure 4-6. Velocity Vector Plot of 90 kW Simulation after 1 Hour Runtime

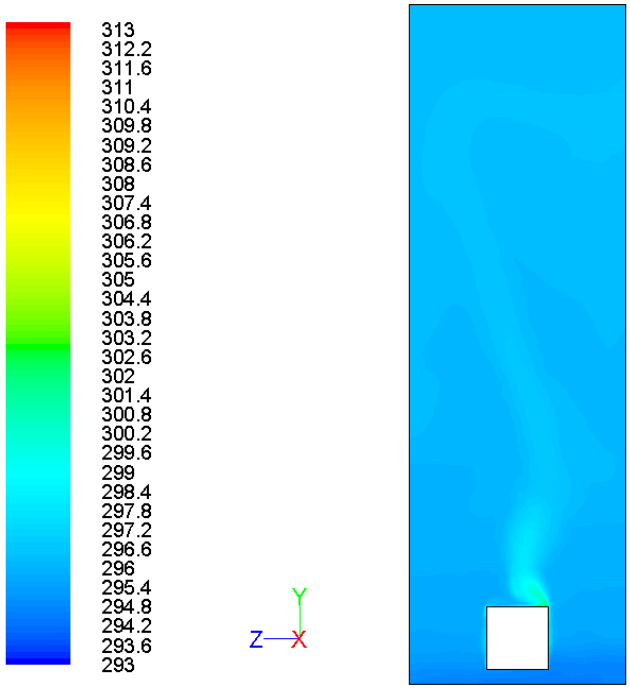

Figure 4-7. Temperature Contour Plot of 100 kW Simulation after 1 Hour Runtime

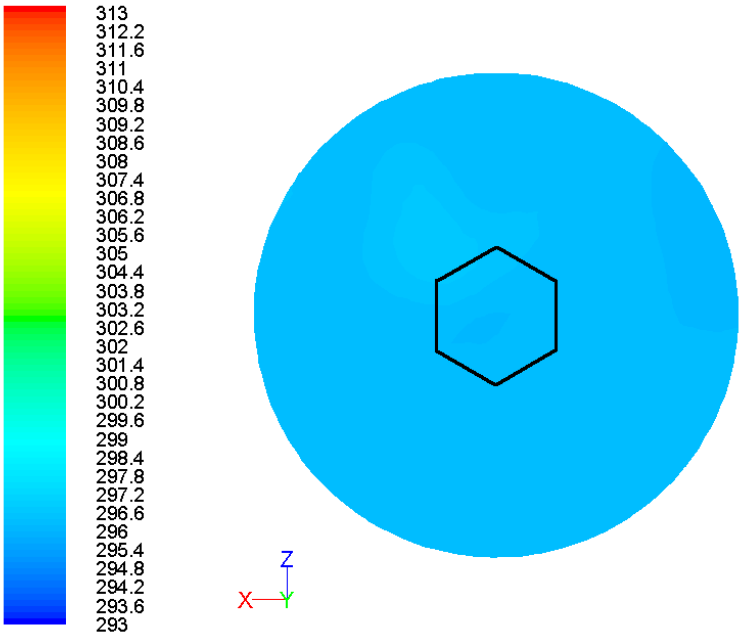

Figure 4-8. Temperature Contour Plot of 100 kW Simulation after 1 Hour Runtime, 4.5 meter Plane

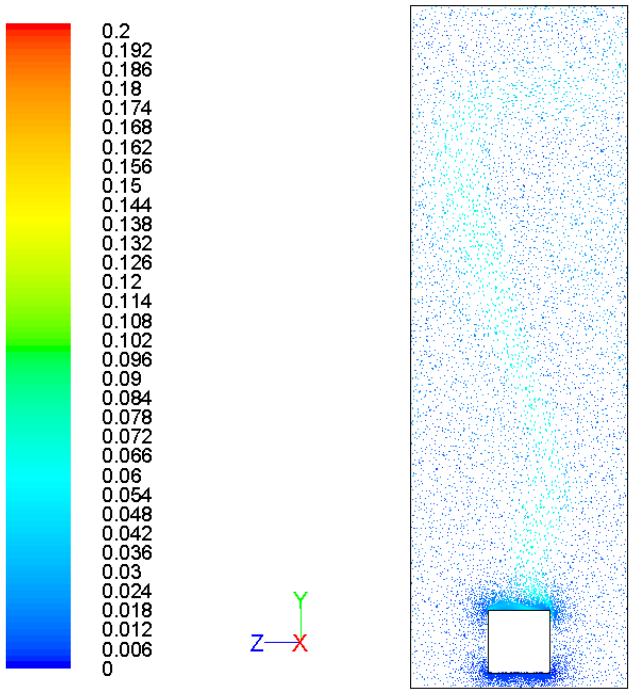

Figure 4-9. Velocity Vector Plot of 100 kW Simulation after 1 Hour Runtime

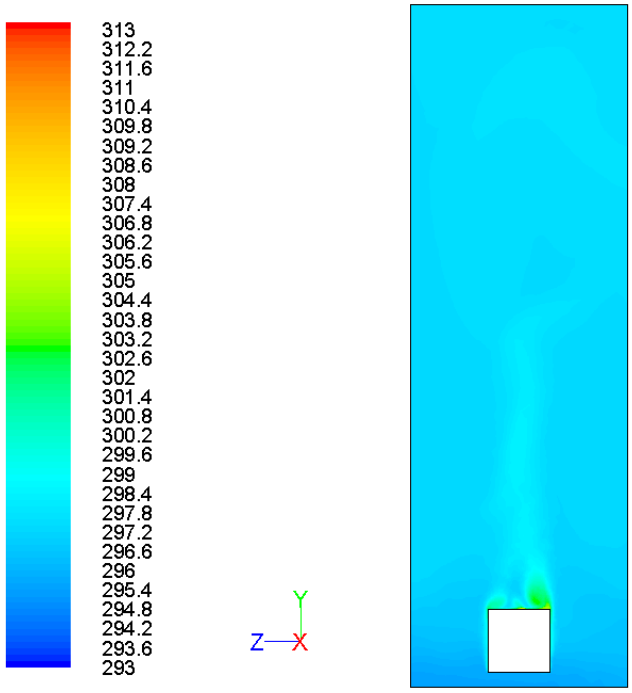

Figure 4-10. Temperature Contour Plot of 150 kW Simulation after 1 Hour Runtime

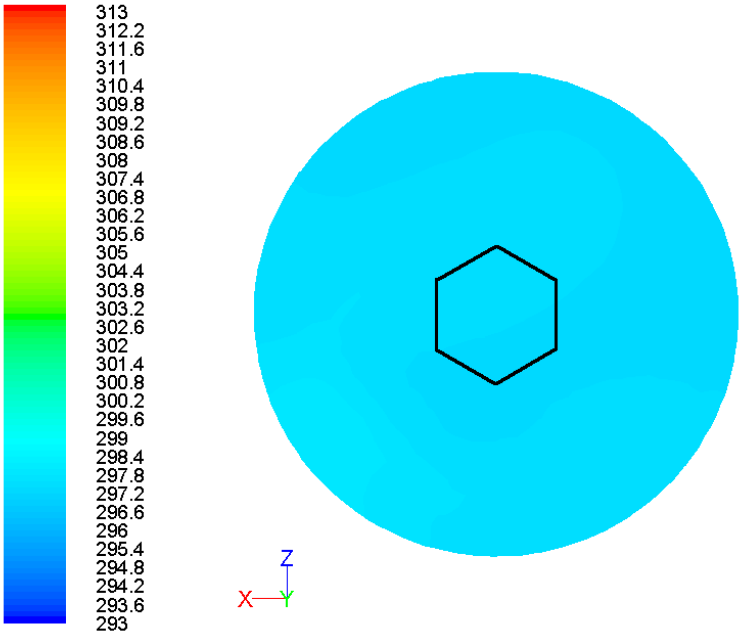

Figure 4-11. Temperature Contour Plot of 150 kW Simulation after 1 Hour Runtime, 4.5 meter Plane

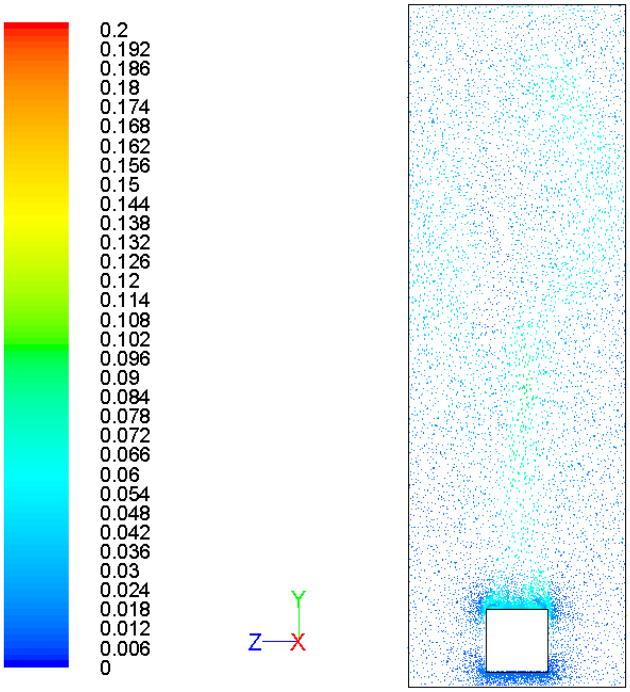

Figure 4-12. Velocity Vector Plot of 150 kW Simulation after 1 Hour Runtime

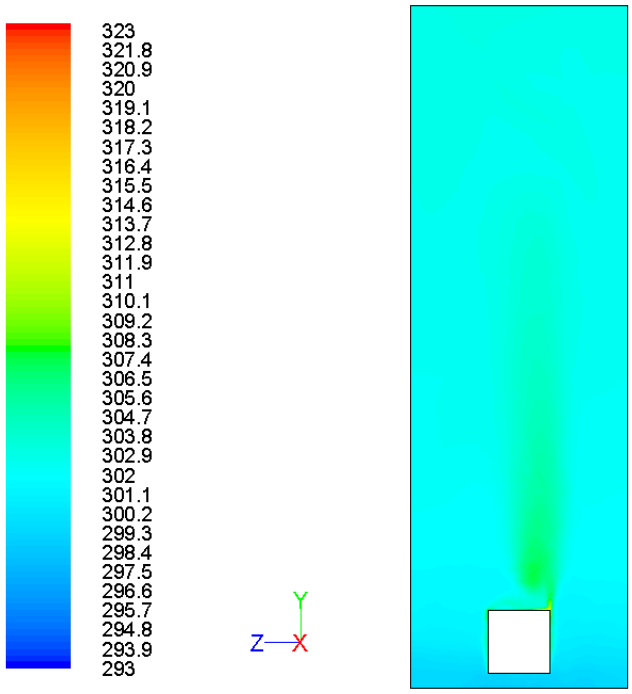

Figure 4-13. Temperature Contour Plot of 300 kW Simulation after 1 Hour Runtime

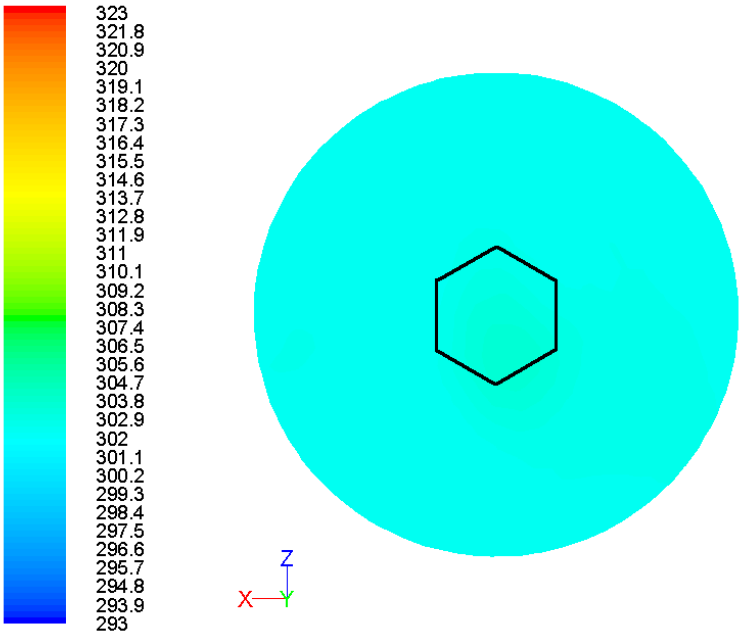

Figure 4-14. Temperature Contour Plot of 300 kW Simulation after 1 Hour Runtime, 4.5 meter Plane

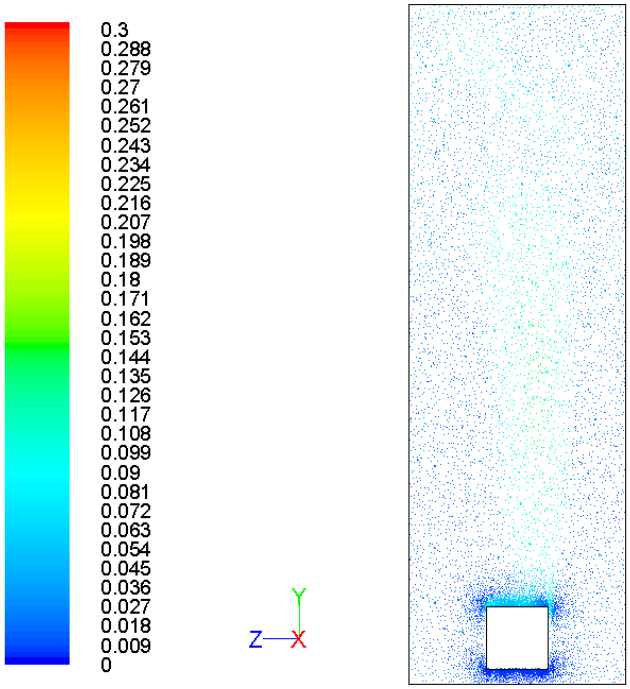

Figure 4-15. Velocity Vector Plot of 300 kW Simulation after 1 Hour Runtime

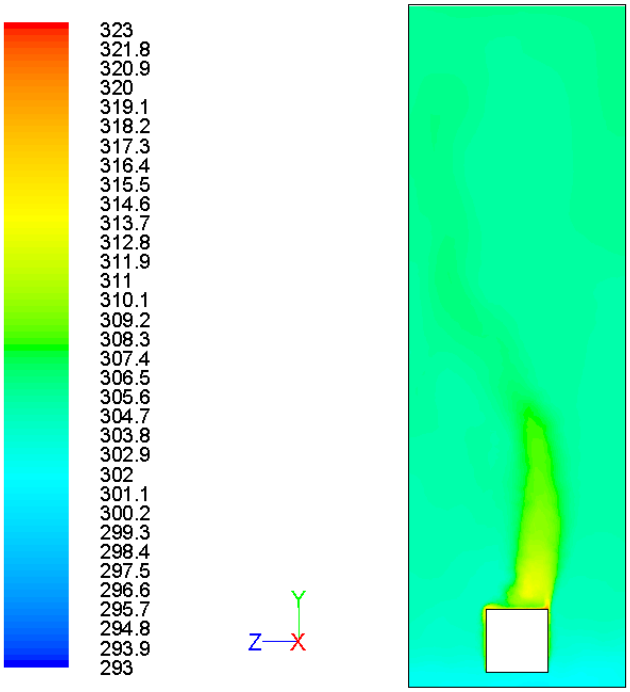

Figure 4-16. Temperature Contour Plot of 400 kW Simulation after 1 Hour Runtime

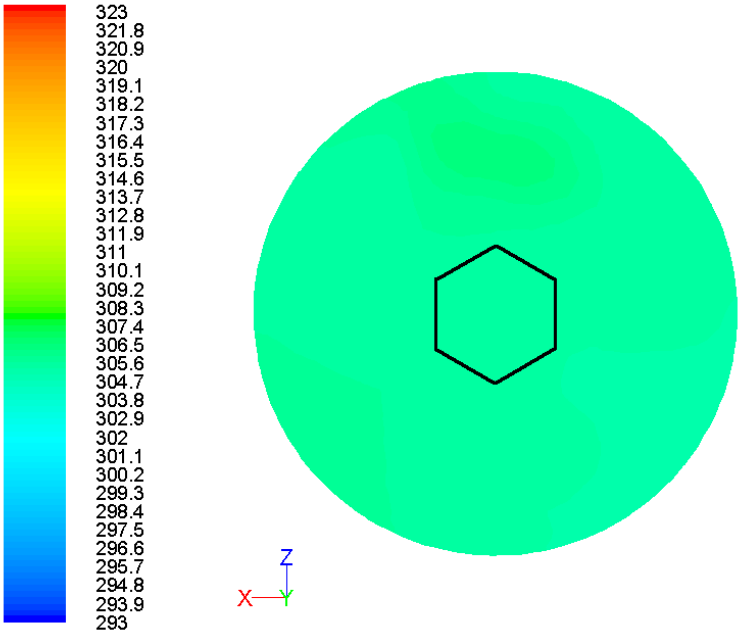

Figure 4-17. Temperature Contour Plot of 400 kW Simulation after 1 Hour Runtime, 4.5 meter Plane

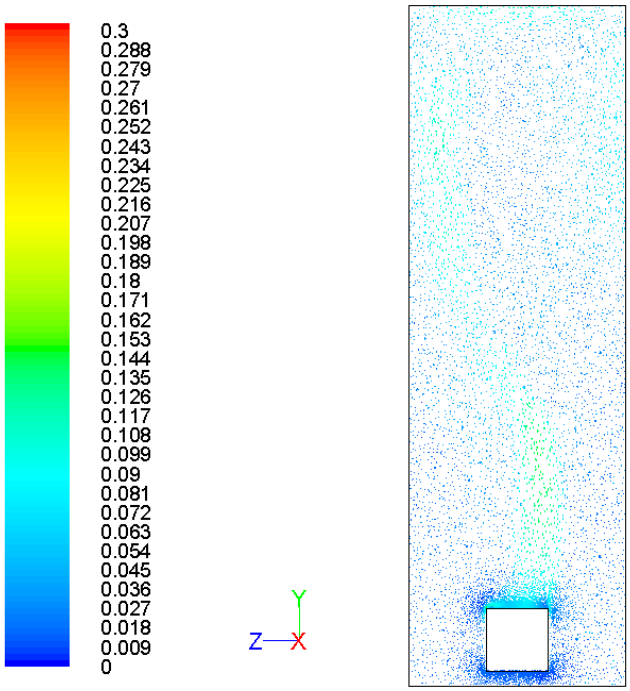

Figure 4-18. Velocity Vector Plot of 400 kW Simulation after 1 Hour Runtime

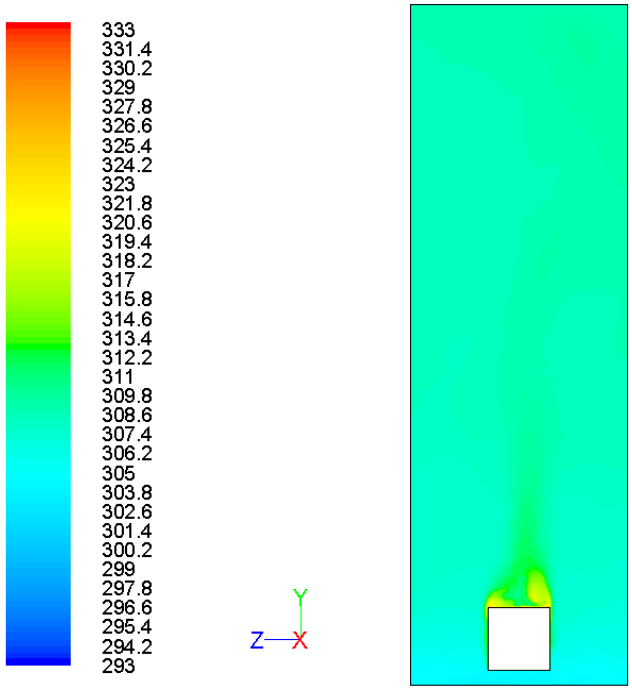

Figure 4-19. Temperature Contour Plot of 500 kW Simulation after 1 Hour Runtime

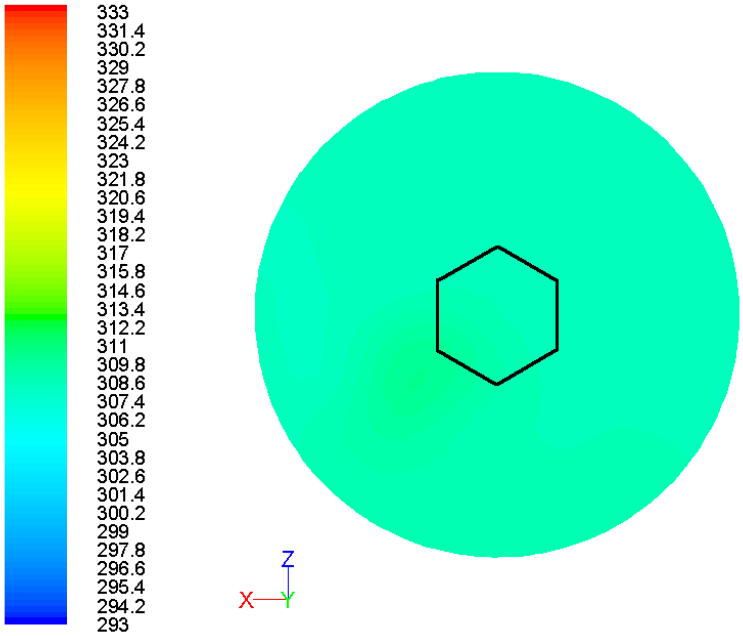

Figure 4-20. Temperature Contour Plot of 500 kW Simulation after 1 Hour Runtime, 4.5 meter Plane

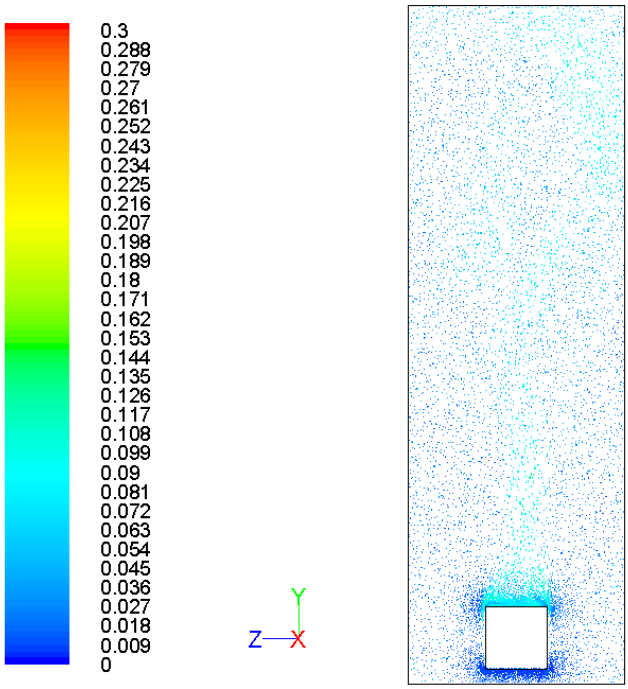

Figure 4-21. Velocity Vector Plot of 500 kW Simulation after 1 Hour Runtime

Table 4-1. Fluent Mesh Statistics

Type	Number
Cells	329,024
Faces	668,208
Nodes	60,094
Face Zones	22

Table 4-2. Fluent Material Properties

Material	Density (kg/m^3)	Viscosity (Pa-s)	Specific Heat (J/kg-K)	Thermal Conductivity (W/m-K)
Aluminum	2,719	-	871	202.4
Water (liquid)	998.2	0.001003	4,182	0.6

Table 4-3. Fluent 1 Hour Runtime Simulation Temperature Results

Reactor Power (kW)	Temp rise at center (°C)	Temp rise at core edge (°C)	Temp rise at 1/2 distance (°C)	Temp rise at tank wall (°C)
90	2.5	2.7	2.5	2.5
100	3.3	3.3	3.2	3.0
150	4.5	4.3	4.3	4.3
300	10.4	9.7	9.7	9.4
400	12.4	12.4	12.4	12.2
500	16.2	16.9	15.3	15.0

CHAPTER 5

COMPARISON OF RESULTS AND MEASUREMENTS

5.1 Introduction

Chapters 3 and 4 showed the results from the SolidWorks and Fluent simulations of the UUTR of various power levels. In this chapter these simulation results are compared and discussed. In addition, temperature measurement data from UUTR reactor runs are presented and compared to the simulations.

5.2 Simulation Results Comparison

Three power levels were the same in these two simulations: 90, 100 and 150 kW. In Figure 5-1, a Fluent and SolidWorks comparison of the center temperatures at the 4.5 meter plane is shown. It can be observed that SolidWorks always produced a higher temperature value. The highest temperature difference is obtained for the UUTR at 90 kW with a difference of 0.36°C or 1.6%. The small difference at the 100 kW level and overall variability between the two data sets is attributed to the location of the natural convection current. When the warmer fluid in the convection current is in the area where the simulation results are taken the temperature recorded is higher than the average fluid temperature. If the point where the results are taken is outside the convection current the temperature is near the average fluid temperature.

The two models both show the near constant upward slope of increasing temperature versus reactor power as expected. The Fluent model shows more variation since the core was discretized according to fuel element levels. The asymmetrical layout of the core leads to a more unstable and mobile convection column causing more variation in the temperature results. The SolidWorks model used a constant, volume type power source and thus had less water movement with a more stable, uniform convection column. The Fluent model more accurately models the actual water flow while the SolidWorks model better shows the overall average temperature.

5.3 UUTR Temperature Measurements

The UUTR pool water temperature is measured with the readings taken at 4.5 meter (14.76 foot) distance from the bottom of the reactor pool and at the predetermined radial distances as shown in Figure 5-2. The side chosen for the edge measurements was near fuel element location G-19 because of its higher flux and ease of measurement access. During normal 90 kW reactor operations three temperature measurements were taken: during startup, after 30 minutes runtime, and after 1 hour runtime. A type K thermocouple attached to an Omega TrueRMS Super Meter was used for collecting all the data. The thermocouple was lowered into the desired position, allowed to acclimate for 1 minute and then the detected temperature range was recorded. Before use the Omega Super Meter was calibrated using the Omega Instruments thermocouple calibration meter and was found to be operating normally.

The results from the pool water measurements are summarized in Tables 5-1 and 5-2 (Note: the first trial was only conducted in the central location). All of the

measurements show some variation between readings. This variation is caused by the following four reasons:

- The first and most important is the location of the convection current. The flow around the core begins to exhibit vortex shedding once it has developed. This moves the convection current of heated water back and forth around the middle area of the reactor pool (as can be evidenced in the Fluent results in Chapter 4). If the thermal column is away from the point of measurement at the time readings are taken the temperature will be lower since the surroundings were measured and not the heated water directly from the core.
- The temperature is also affected by the humans measuring and operating the UUTR. At UUTR the reactor power is manually controlled by the operator. While each trial was conducted at 90 kW there is slight variation. Because of this, it is easy to expect a variation of 90±1 kW. Over longer periods of time small changes in the power can create slight differences in the temperature between the measurements.
- The operator also controls the rate the reactor power is increased before reaching the level of 90 kW. Ideally the power would be ramped to the desired level instantaneously. However, in practice this operation can take a few minutes or longer depending on the current conditions and experiments conducted. This time spent ramping up to power still increases tank water temperature and has an effect on the temperature measurements.

- Finally, the temperature is affected by the ambient starting conditions. During the summer the reactor room temperature is higher causing the starting pool water temperature to also be higher. From freezing to 35°C the water's heat capacity (C_p) slightly decreases, making it easier to heat. This is evidenced in the two starting temperatures (20°C and 24°C) of both the SolidWorks and Fluent simulations where the 90 kW, 24°C simulation more closely matches the measurements taken.

5.4 Simulation and Temperature Measurement Comparison

Currently only results from the 90 kW power level are comparable among the simulations and measurements. Table 5-3 summarizes these results. There is close correlation between both of the models used and the actual measurements. Since the actual measurements were taken during the summer months when ambient temperature is higher the 24°C simulations are a closer approximation then the 20°C simulations. The temperature range between the data can be attributed to the location of the convection current as discussed previously. Because the Fluent simulations contain a more accurate model of the asymmetrical core the convection current is more obvious. It is also expected that not every measurement would capture readings from the inside the convection current. These results show that a series of measurements are necessary to gauge the temperature rise in UUTR and that while it local variability is seen overall the temperature rise follows predictable trends.

5.5 UUTR of Higher Power Levels

The simulation of UUTR at higher power levels show that the reactor undergoes the same natural convective cooling process only the effects become more pronounced. In the 90 kW simulation the open water fluid velocity peaked at 0.0988 m/s while in the 500 kW simulation the maximum velocity has increased to 0.156 m/s. These results are similar, only more conservative, to those reported in the SAR which reports 0.115 m/s for 90 kW and 0.130 m/s for 100 kW [1]. The slower velocities can be attributed to the simpler reactor core models used in both simulations. These models did not include the coolant channels through the center of the reactor and around each element. If these channels were included additional convection heating would occur increasing the velocities.

The other aspect that is seen in the simulations and becomes more pronounced at higher power levels is the vortex shedding in the convection current above the reactor core. Because of its asymmetrical power distribution and acting as a blunt body in the flow field the core creates vortices that travel up the convection column. The vortices cause the movement of the convection column around the reactor pool. As the convection current and velocities increase with higher power levels the vortices also grow and affect the current to a greater extent.

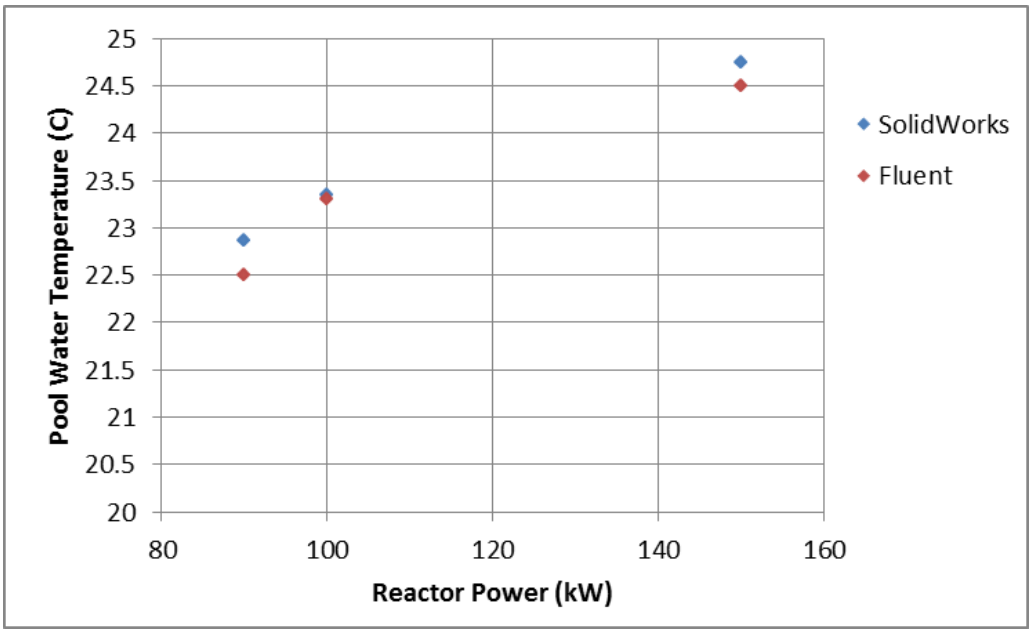

Figure 5-1. Comparison of SolidWorks and Fluent Centerline Temperatures on the 4.5 meter Plane

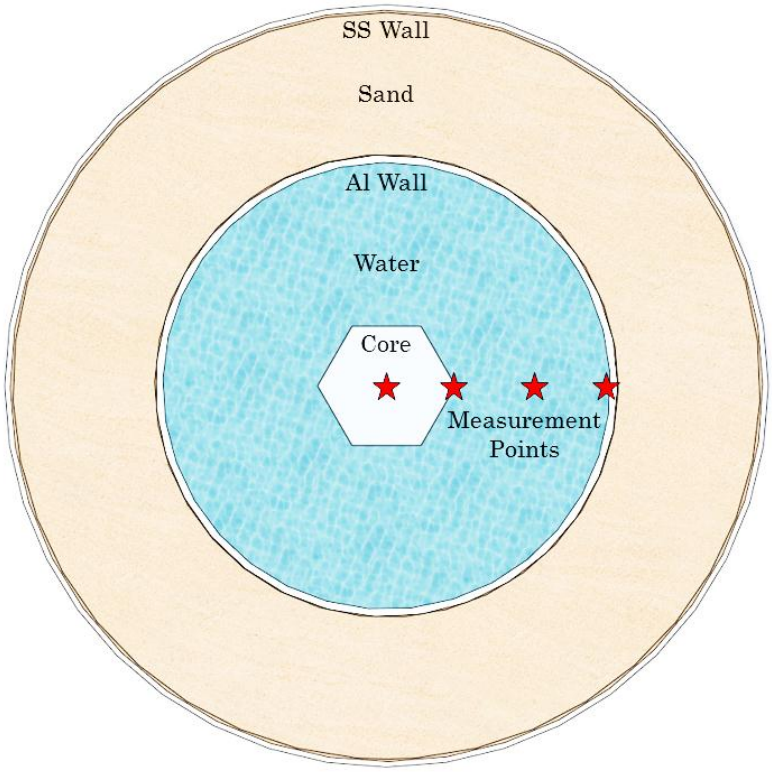

Figure 5-2. Radial Locations of Temperature Measurements in the UUTR

Table 5-1. UUTR Pool Temperature Measurements at 90 kW after 30 Minutes

Point	Distance from Center (m)	Temp Rise, 3/29/12 (°C)	Temp Rise, 4/5/12 (°C)	Temp Rise, 5/29/12 (°C)	Temp Rise, 7/28/12 (°C)	Temp Rise, 8/8/12 (°C)
1 (C.I.)	-	1.3±0.7	1.0±0.3	1.2±0.2	1.3±0.2	1.4±0.3
2 (Core Edge)	0.34	-	1.5±0.1	1.5±0.2	1.3±0.1	1.4±0.3
3 (1/2 Distance)	1.08	-	1.4±0.1	1.5±0.2	1.4±0.1	1.5±0.2
4 (Tank Wall)	2.15	-	1.4±0.1	1.4±0.1	1.4±0.1	1.5±0.1

Table 5-2. UUTR Pool Temperature Measurements at 90 kW after 1 Hour

Point	Distance from Center (m)	Temp Rise, 3/29/12 (°C)	Temp Rise, 4/5/12 (°C)	Temp Rise, 5/29/12 (°C)	Temp Rise, 7/28/12 (°C)	Temp Rise, 8/8/12 (°C)
1 (C.I.)	-	2.5±0.5	2.9±0.1	2.8±0.3	3.2±0.4	3.0±0.3
2 (Core Edge)	0.34	-	2.4±0.2	3.0±0.2	3.1±0.2	2.9±0.2
3 (1/2 Distance)	1.08	-	2.8±0.1	2.7±0.1	2.8±0.1	2.8±0.1
4 (Tank Wall)	2.15	-	2.7±0.1	2.7±0.1	2.7±0.1	2.8±0.1

Table 5-3. Comparison of Simulation and Temperature Measurements at 90 kW

	C.I. Point Temp Rise (°C)	Core Edge Temp Rise (°C)	1/2 Distance Temp Rise (°C)	Tank Wall Temp Rise (°C)
UUTR 3/29/12	2.5±0.5	-	-	-
UUTR 4/5/12	2.9±0.1	2.4±0.2	2.8±0.1	2.7±0.1
UUTR 5/29/12	2.8±0.3	3.0±0.2	2.7±0.1	2.7±0.1
UUTR 7/28/12	3.2±0.4	3.1±0.2	2.8±0.1	2.7±0.1
UUTR 8/8/12	3.0±0.3	2.9±0.2	2.8±0.1	2.8±0.1
Fluent (20°C)	2.54	2.73	2.51	2.50
SolidWorks (20°C)	2.86	2.90	2.82	2.80
Fluent (24°C)	3.11	2.98	2.97	2.73
SolidWorks (24°C)	2.96	2.95	2.90	2.68

CHAPTER 6

DEPARTURE FROM NUCLEATE BOILING RATIO

6.1 Introduction

This chapter describes the departure from nucleate boiling in UUTR in showing that even at higher power levels the heat flux needed to cause this phenomenon is not reached. To model the fuel element heat flux at higher power levels the PARET code [17] from Argonne National Lab is used.

6.2 Background

When heat is applied to a surface (in this case a fuel element) in saturated water the heat flux transferred to the water begins to steadily increase. This increase continues as boiling begins and up to the point of steady nucleate boiling. After the point of nucleate boiling the heat transfer to the water quickly decreases as film boiling begins and the layer of steam prevents water from contacting the surface. Reaching this stage is known as burnout since the quickly decreased heat transfer rate and increased temperatures can damage or melt reactor fuel. The surface heat transfer rate is shown plotted in Figure 6-1 and is known as the Nukiyama Curve.

The departure from nucleate boiling ratio (DNBR) is a ratio of the critical heat flux (CHF) needed to cause departure from nucleate boiling to the actual heat flux

on the fuel element. The DNBR is dependent on the coolant velocity, the pressure and the extent the fluid is below the saturation temperature. For fuel safety it is recommended that the DNBR for TRIGA reactors not be below 1.0 [1, 18] whereas in commercial PWR reactors the minimum design value is 1.3 [20].

6.3 Calculation of the Critical Heat Flux

The first step in finding the DNBR is the calculation of the CHF. Actual, accurate CHF data is difficult to obtain so a conservative correlation is used to supply the needed information. For TRIGA reactors the accepted, traditional method is using the Bernath Correlation [5, 19]:

$$CHF = h_{crit}\left(T_{crit} - T_f\right) \tag{6.1}$$

$$h_{crit} = 61.84\left(\frac{D_w}{D_w + D_i}\right) + \left(0.01863\left(\frac{23.53}{D_w^{0.6}}\right)u\right) \tag{6.2}$$

$$T_{crit} = 57\ln p - \left(\frac{54P}{P+0.1034}\right) + 283.7 - \frac{u}{1.219} \tag{6.3}$$

where CHF is critical heat flux (W/m^2)

h_{crit} is critical coefficient of heat transfer (W/m^{2}K)

T_{crit} is critical surface temperature (°C)

T_f is bulk fluid temperature (°C)

p is pressure (MPa)

u is fluid velocity (m/s)

D_w is wet hydraulic diameter (m)

D_i is diameter of the heat source (m)

From MCNP5 simulation it is found that the fuel element with the highest power is located in the B-ring. For calculating the CHF the most conservative geometry for this location is used [1]. Figure 6-2 shows the sub-channel geometry. All the values used to calculate the CHF are presented in Table 6-1 and are shown for a starting fluid temperature of 20°C.

The CHF as given by Bernath's Correlation is displayed in Figure 6-3 for reactor powers of 90, 100, 150, 300, 400 and 500 kW. The CHF values shown in Figure 6-3 are based on inlet temperature, when DNB is expected to occur. The CHF is also presented using Bernath's Correlation as a function of coolant flow rate in Figure 6-4. Coolant flow rates of 0.05, 0.075, 0.1, 0.15, 0.25, 0.5, 0.75 and 1 m/s are shown plotted.

6.4 Calculation of the Departure from Nucleate Boiling Ratio

Knowing the critical heat flux when DNB is expected to occur, the actual heat flux under the same conditions is then required. The ratio of these two values forms the departure from nucleate boiling ratio.

$$DNBR = \frac{Critical\ Heat\ Flux}{Actual\ Heat\ Flux} \tag{6.4}$$

The PARET (Program for the Analysis of REactor Transients) code from Argonne National Laboratory is used to model the heat flux for UUTR.

PARET predicts and simulates conditions and nondestructive accidents in research and test reactors [17]. Using inputs based on UUTR's design and configuration the program is used to model the steady-state thermodynamic

conditions including coolant and fuel temperatures, and heat flux. These are modeled for both the hottest and nominal fuel elements.

Table 6-2 shows the main input parameters used in the PARET code with the full version of the code being included in Appendix D. The PARET code provides information such as axial profiles of moderator temperature, fuel element temperature and fuel element surface heat flux. Only the maximum surface heat flux from the hottest fuel element is of interest for the DNBR calculation and is shown in Table 6-3.

The CHF is read from the plots generated using Bernath's Correlation in Figure 6-3. The UUTR Technical Specifications require that the pool water temperature be no higher than 35°C [1] so the CHF is read at this temperature by finding the point at which each power level intersects the 35°C line. The resulting critical heat fluxes and departure from nucleate boiling ratios are shown in Table 6-4.

6.5 UUTR Boiling Analysis

The DNBR calculation shows that using Bernath's Correlation and maximum heat flux data from the PARET code that a boiling crisis will not occur even if the UUTR's power is upgraded to 500 kW. Currently, during 90 kW operations there is no boiling on any of the reactor fuel elements. Based only on the absolute pressure at the bottom of the reactor tank the boiling point of the tank water would be elevated to 127.5°C. PARET factors into account the coolant flow rate and calculates a new temperature for the start of DNB. This is displayed for the hottest fuel channel in Table 6-5 and is compared to the highest fuel cladding surface temperature calculated.

The DNB temperature is a function of the coolant flow rate, increasing or decreasing as the rate speeds up or slows down respectively. The coolant flow rate is driven by the natural convection current and increases as the heat flux and reactor power increase. However, the increase in the heat flux with higher reactor powers outpaces the increase in the coolant flow rate leading to the cladding surface temperature meeting the DNB temperature of 131.9°C when the reactor is operating at 210 kW. After this point the boiling is still in a nucleate regime but this shows that the inflection point shown on Figure 6-1 has been reached. The 500 kW PARET simulation shows that the boiling remains in this state and does not increase above the CHF.

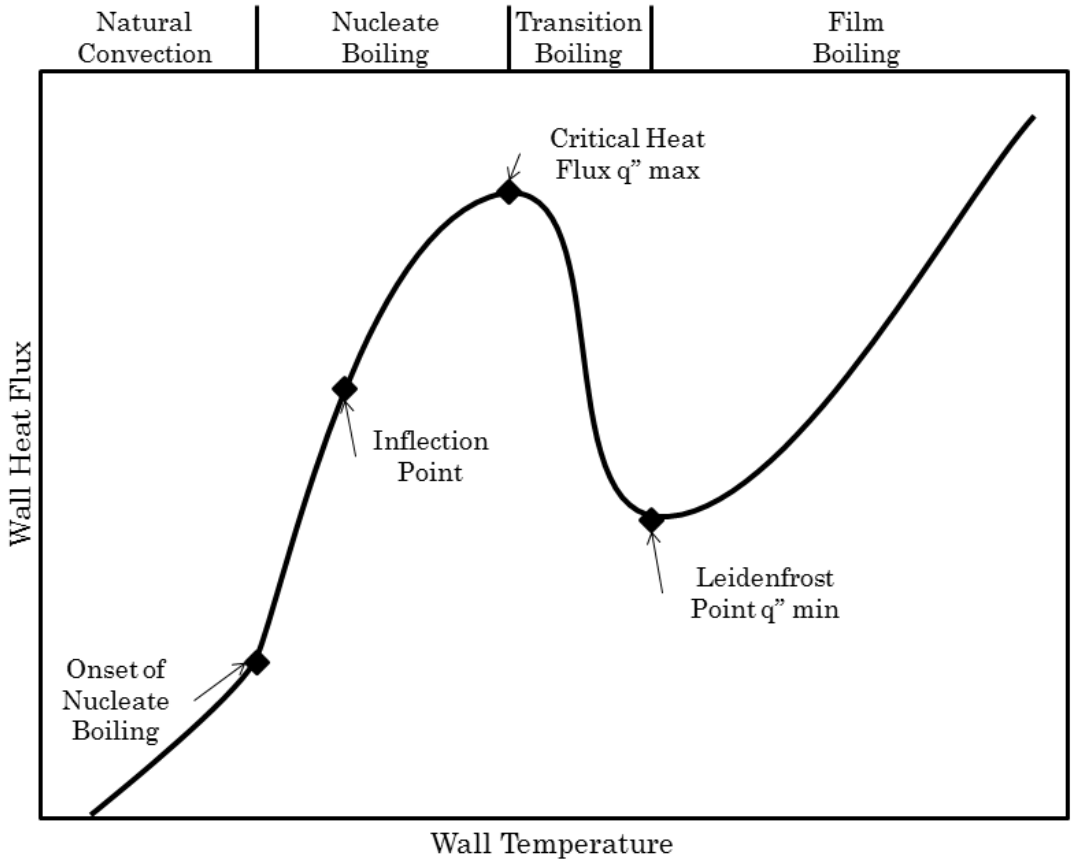

Figure 6-1. The Boiling Curve for Saturated Water at Standard Pressure

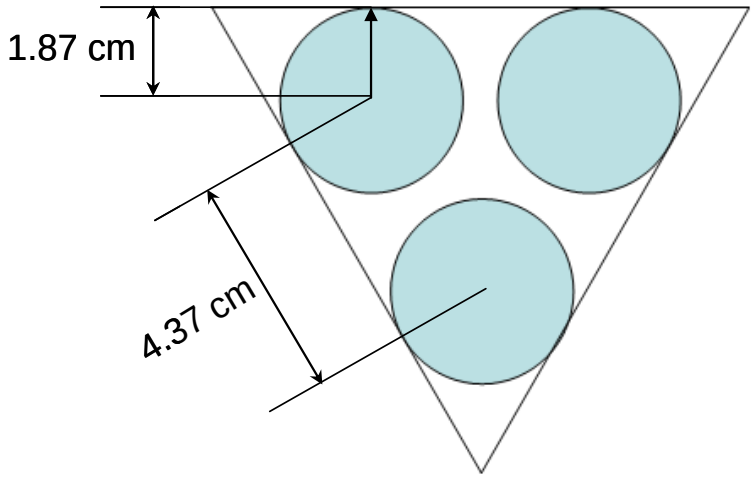

Figure 6-2. Hottest Fuel Element Subchannel Geometry [1]

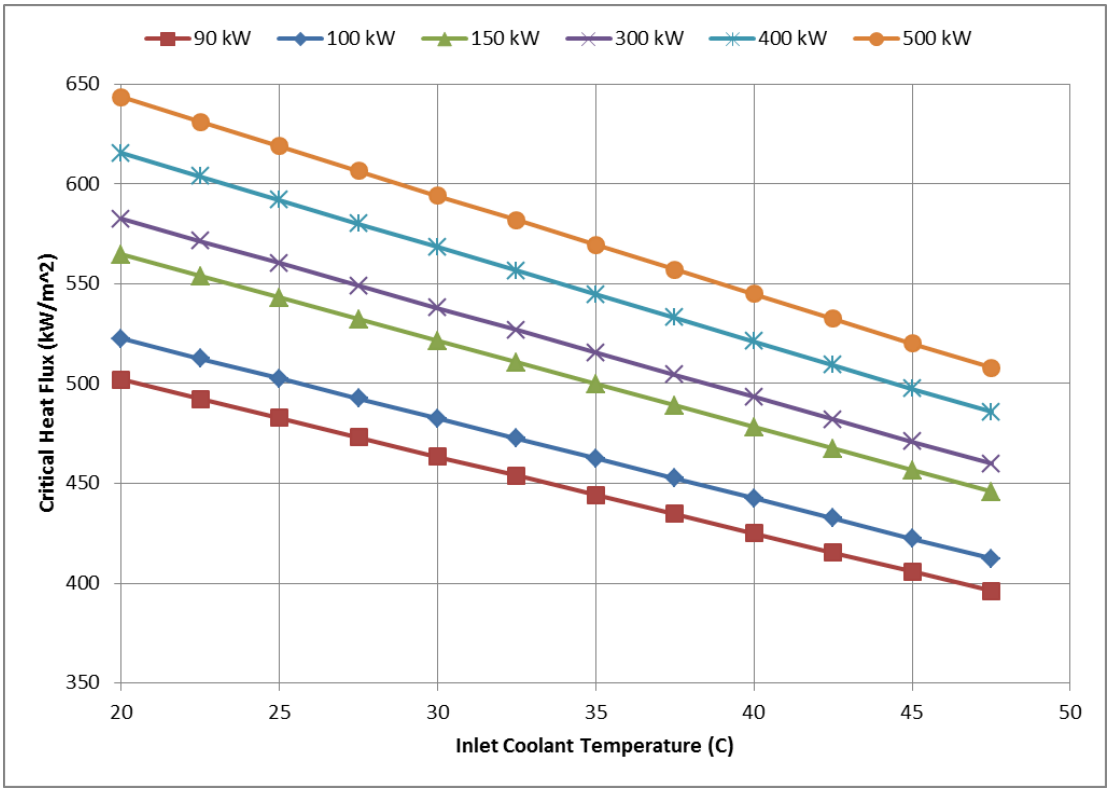

Figure 6-3. CHF Calculated Using Bernath's Correlation as a Function of Coolant Inlet Temperature for Various Reactor Powers

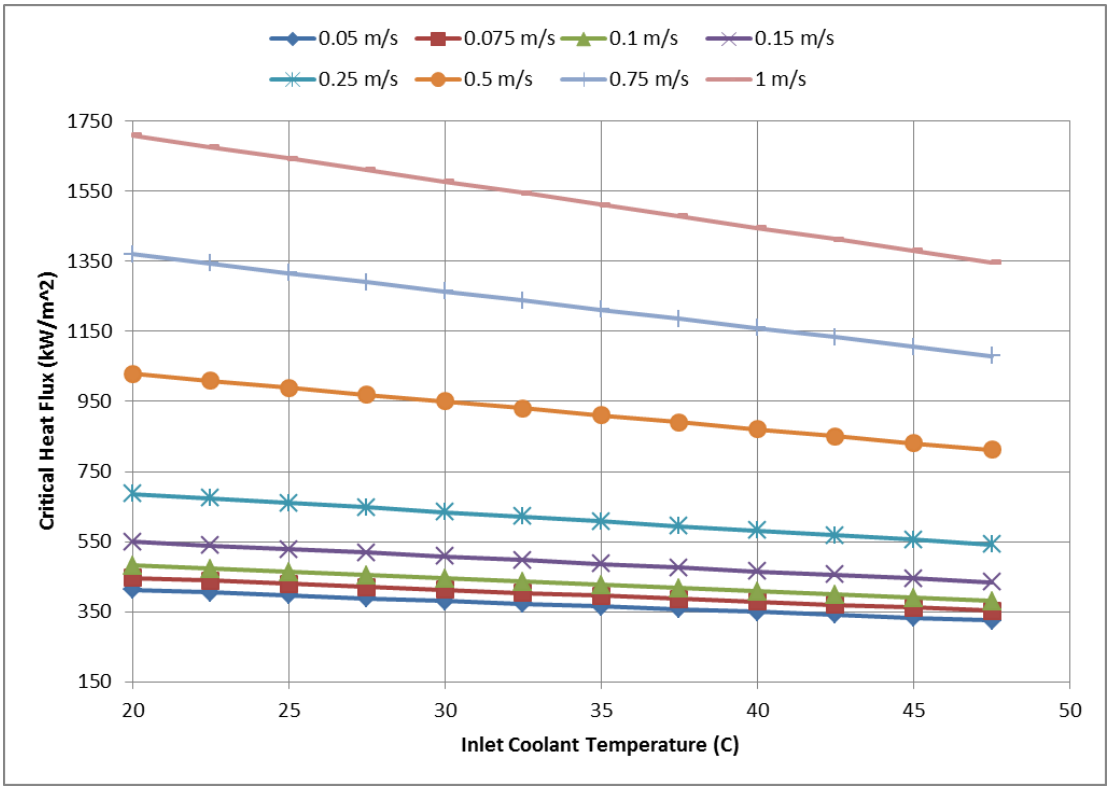

Figure 6-4. CHF Calculated Using Bernath's Correlation as a Function of Coolant Inlet Temperature and Coolant Flow Rate

Table 6-1. Values Used in Calculating the Critical Heat Flux

Variable	90 kW	100 kW	150 kW	300 kW	400 kW	500 kW
h_{crit} (W/m^{2}K)	3.847	4.001	4.329	4.467	4.720	4.935
T_{crit} (°C)	150.487	150.477	150.449	150.439	150.419	150.402
T_f (°C)	20.0					
p (MPa)	0.176					
u (m/s)	0.115	0.130	0.161	0.174	0.198	0.218
D_w (m)	0.00499					
D_i (m)	0.112					

Table 6-2. Main PARET Input Parameters

Variable	90 kW	100 kW	150 kW	300 kW	400 kW	500 kW
Inlet Moderator Temp (°C)	20.6					
Fuel Pin Radius (m)	1.792 x10^{-2}					
Thermal Conductivity UZrH (W/m-K)	18.0					
Thermal Conductivity Air Gap (W/m-K)	0.199					
Thermal Conductivity S.S. Clad (W/m-K)	16.8					
Axial Neutron Flux Ratio	Data for each power level provided from [1, 16]					
Moderator Inlet Mass Velocity (kg/s-m^2)	115	130	158	179	202	218

Table 6-3. PARET Calculated Maximum Surface Heat Flux

UUTR Power Level	Maximum Heat Flux (W/m^2)
90 kW	44,419
100 kW	49,057
150 kW	74,032
300 kW	148,064
400 kW	197,419
500 kW	246,774

Table 6-4. UUTR Critical Heat Flux and DNBR at 35°C

Power Level	Critical Heat Flux (kW/m^2)	DNBR
90 kW	444.2	10.00
100 kW	462.5	9.43
150 kW	499.8	6.75
300 kW	515.6	3.48
400 kW	544.7	2.76
500 kW	569.5	2.31

Table 6-5. PARET Hottest Element Calculated DNB and Cladding Surface Temperatures

Power Level	DNB Temperature (°C)	Cladding Surface Temperature (°C)
90 kW	130.93	100.88
100 kW	131.25	101.45
150 kW	131.77	124.00
300 kW	132.10	133.43
400 kW	132.44	134.80
500 kW	132.66	135.93

CHAPTER 7

HIGHER POWER UUTR COOLING SYSTEM DESIGN

7.1 Introduction

Extended operations of the UUTR at higher power levels necessitate the need of a new cooling system. Similar upgrades and costs are investigated at other research facilities [21, 22, 23 and 24]. For the UUTR two systems are proposed: a low-cost component upgrade and a complete new design. Costs, materials and the benefits of both proposals are compared.

7.2 Review of the Upgrades at Other Facilities

Reactor modernization and refurbishment is not uncommon among research reactors and often includes upgrades increases to the power and cooling system [21]. TRIGA reactor upgrades in Brazil, Indonesia and at Oregon State University are analyzed for their upgrades and described in brief as follows.

The IPR-R1 TRIGA Mark I reactor in Belo Horizonte, Brazil was upgraded from 30 kW to 250 kW in 1970 [22]. This system was most similar to UUTR because of the presence of a 30 kW refrigeration cooling system attached to the water purification loop. The purification loop was kept in place for use in the new system. All piping was replaced with stainless steel and underground conduits were dug for piping connections to the outside cooling tower. The heat exchanger

was a shell and tube type designed for an input temperature of 40.7°C and an output of 33.1°C with a mass flow rate of 30,000 kg/hr. The cooling tower was designed for a wet bulb temperature of 24.4°C and a flow rate of 40,000 kg/hr. Installation was done in parallel with reactor operations with a maximum shutdown time of two days. Total costs were calculated to be $225,000 (in 2012 dollars) [22].

The Bandung TRIGA Mark II reactor in Bandung, Indonesia completed a power and cooling system upgrade from 1,000 kW to 2,000 kW in the year 2000 [23]. During the retrofit nearly all reactor components were upgraded including: the core, a new tank and a new primary and secondary cooling system. The new system was built with a plate type heat exchanger connected to two cooling towers located outside. Both were rated to 2,400 kW of cooling load and were designed and built locally by the Nuclear Technology Center. One million dollars was budgeted for the design, construction and building of the new cooling, ventilation and I & C systems. The complete upgrade took four years to finish.

The Oregon State TRIGA reactor in Corvallis, Oregon has also undergone a similar upgrade [24]. In 1970 the reactor was upgraded from 250 kW to 1 MW. A 1 MW shell and tube heat exchanger linked to a cooling tower was installed over seven months in 1971. A new coolant flow rate of 350 gpm was measured. Some observations were made after the installation: radiation levels decreased on the top of the reactor tank by two to three times, a low resonance vibration can sometimes be detected in the core and radiation levels in the demineralizer have increased eight times. It is believed that the radiation level decrease is due to the higher flow rate allowing less N-16 to reach the surface while the higher level is caused by increased sediment from the bottom of the tank getting picked up and trapped in

the demineralizer. The vibration detected was found to be caused by nucleate boiling taking place on the fuel elements.

7.3 UUTR Low-Cost Upgrade

Without any core or reactor modifications it is found that the maximum UUTR power level is 150 kW [16]. UUTR does not operate at this level as only two hours and six minutes of runtime would be available if started at 20°C before the internal temperature limit of 30°C would be reached. This limit is set to avoid the Technical Specifications limit of 35°C that protects the integrity of the deionizing resin beds. At higher temperatures the resin integrity begins to degrade leaching the removed contaminates back into the water.

Recently, higher grade, more temperature resistant deionizing resins have become widely available for less cost. Manufacturers such as ResinTech® and Purolite® both make products that fit in this category [25, 26]. The ResinTech® MBD-10 nuclear grade, mixed bed resin functions up to 60°C if rechargeable and up to 80°C if single use and meets all other water quality requirements [27]. In a telephone interview conducted with a local water equipment supplier the cost of a new, higher grade deionizing resin was estimated at $3,000-$5,000 and could be installed with minimal effort [28].

To extend the operating time and increase the operating power of UUTR for minimal cost it is recommended that one of these new deionizing beds be installed and the Technical Specifications be amended to have a water temperature limit of 45°C. Operating under these conditions the new internal temperature limit would be set at 40°C. This increase in temperature limit would allow three and a half additional hours of operating time at 90 kW or two hours and ten minutes

additional time if upgraded and operating at 150 kW. Figure 7-1, based off of the previous simulations conducted, illustrates the theoretical runtimes for various power levels when starting at 20°C.

This upgrade only retrofits UUTR for higher temperature operations and does not provide any additional cooling capabilities. UUTR would still be cooled through natural heat transfer to the surroundings. Because of this extra shutdown time would be required following higher temperature runs to allow for ambient cooling. Based on the current schedule of UUTR activity with two to three runs per month this should not be an issue.

7.4 UUTR Complete Cooling System Replacement

To enable longer, more frequent UUTR runtimes with an increase in power level a new cooling system needs to be considered. A dual-loop system connected through a heat exchanger and routed to an outdoor cooling tower is commonly used to cool research reactors and would be best suited for UUTR. A basic piping and instrumentation diagram for a theoretical UUTR system is shown in Figure 7-2.

For the sole purpose of estimating the costs of a cooling system UUTR is assumed to be operating at 250 kW and the system components are sized appropriately. The theoretical layout in Figure 7-2 would suit any higher power core. Only the size of the heat exchanger, cooling tower, pumps and pipes change as needed. Assuming a 20°C temperature difference in the cooling water from the heat exchanger, a flow rate of 47.4 gpm is required to cool a 250 kW reactor. This assumes no flow losses and is illustrated for other power levels in Figure 7-3.

To supply this flow rate and provide extra head for the losses occurring in the pipes, resin beds and heat exchanger a 5 hp pump is needed costing about $1,500.

These pumps commonly use 2.5 or 3 inch piping connections. Stainless steel, schedule 40 pipe is strong, durable and well suited to this type of operation. It is estimated that 60 feet of piping and fittings are needed for the primary loop and is estimated at $3,000 (use of aluminum piping would be less) [29].

The heat exchanger connects both sides of the cooling loop and is the most important piece in the system. These components are typically manufactured to meet the heat transfer needs of the reactor. Two companies, Alfa Laval and Graham, have experience making heat exchangers for research reactors. In a conversation with the manufacturer it is recommended that a plate heat exchanger be used and would cost approximately $20,000 [30].

The secondary loop supplies cooled water to the heat exchanger from the cooling tower. Because of Utah's dry climate an open circuit cooling tower is the more efficient choice. A 300 kW counter-flow cooling tower is recommended as it allows for maximum heat transfer from the heat exchanger, has a more freeze resistant design for winter use and is commonly available in preassembled units. From conversations with a manufacturer, units of this type are available for $25,000 with about $25,000 more needed to complete the installation [31].

As in the primary loop, the secondary loop also requires a pump and piping network. If the cooling tower is located near the outside wall of the UNEP facility approximately 30 feet of piping would be needed for a cost of $2,000. The cooling tower requires a maximum of 110 gpm of water flow. With the reduced head needed a pump similar to the one in the primary loop can be used for a cost of $1,500. Because the cooling tower is open to the atmosphere, a water treatment system is recommended for the secondary loop to prevent fouling. The manufacturer of the cooling tower says these systems range around $5,000 [31].

To monitor the performance of the system, instrumentation is installed at key points that report to the operator in the control room. Four temperature probes, two per loop, on either side of the heat exchanger are used to monitor the real-time heat transfer. A flow meter is installed in each loop to ensure pump efficiency and monitor flow rates through the deionizers in the primary loop. A Geiger-Muller detector monitors radiation levels in the primary loop that could arise from N-16 production, a fuel cladding leak or activated tank sediment. Two water conductivity probes are installed before and after the deionizing loop to measure their performance and alert the operator for replacement. These probes from the existing system can be reused in the new setup.

In addition to the new hardware there are other installation costs: a site needs to be prepared and concrete laid for the cooling tower, piping needs to be installed and an access panel made through the building to the cooling tower and a second deionizing resin bed is required for increased capacity. The labor associated with the project involves installation, plumbing, wiring and construction work. Based on previous work done at UNEP the average technician labor cost is $100/hour. All work requires at least two technicians present at any time. While completion times vary widely on similar projects at other research reactors, it is estimated that at least one month of installation time be planned. The total estimated cost of the major components of the upgrade is shown in Table 7-1.

A 3-D model of the theoretical, replacement cooling system, including the components described above, was created in SolidWorks. Isometric views of the design are shown in Figures 7-4 and 7-5.

7.5 Combined Upgrade Proposals with Neutronics Simulations

Using neutronics simulation data for a UUTR power upgrade from [16], plots showing the relationship between UUTR power, neutron flux, runtime and cost are displayed to help gauge which proposed upgrade is most suitable. The first scenario, shown in Figure 7-6, assumes that the low-cost upgrade for $5,000 is installed and the UUTR Technical Specifications modified to allow an internal pool water temperature limit of 40°C. The data are from SolidWorks Flow Simulation calculations for the runtime starting at 20°C and timing until 40°C is reached while the total neutron flux is the highest value recorded from MCNP5 simulations. While the low-cost upgrade allows higher temperatures to be reached, the current UUTR core configuration is only capable of 150 kW [16]. To operate at values beyond 150 kW as shown in Figure 7-6 the additional core upgrade outlined in [16] for $115,500 would need to be completed.

If the complete cooling system replacement in 7.4 is completed reactor runtimes are theoretically infinite. In this case the cost of components becomes the defining issue. Figure 7-7 shows the cost of both of the upgrades, the increased power level they provide and the corresponding total neutron flux. The estimated material cost data comes from the projected costs of the UUTR core upgrade and from the costs of the cooling system components. The total neutron flux data is the highest recorded value taken during MCNP5 simulations [16]. The small cost increase between 100 kW and 150 kW is due to the low-cost upgrade for $5,000 being included. This upgrade allows operations up to 150 kW but beyond that the core upgrade is necessary with the cooling system replacement being recommended for 250 kW and above. After 250 kW the price continues to rise as the cooling tower, heat exchanger, pipe and pump size increase proportionally to the power level.

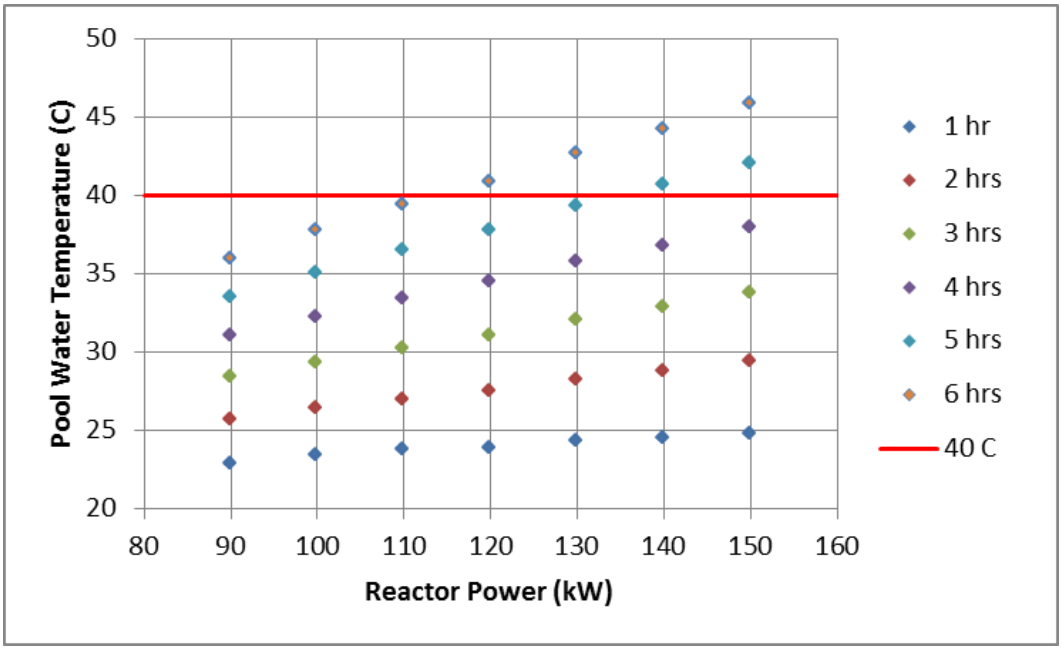

Figure 7-1. UUTR Pool Water Temperature as a Function of UUTR Power after TS Temperature Increase as Obtained with SolidWorks Flow Simulation

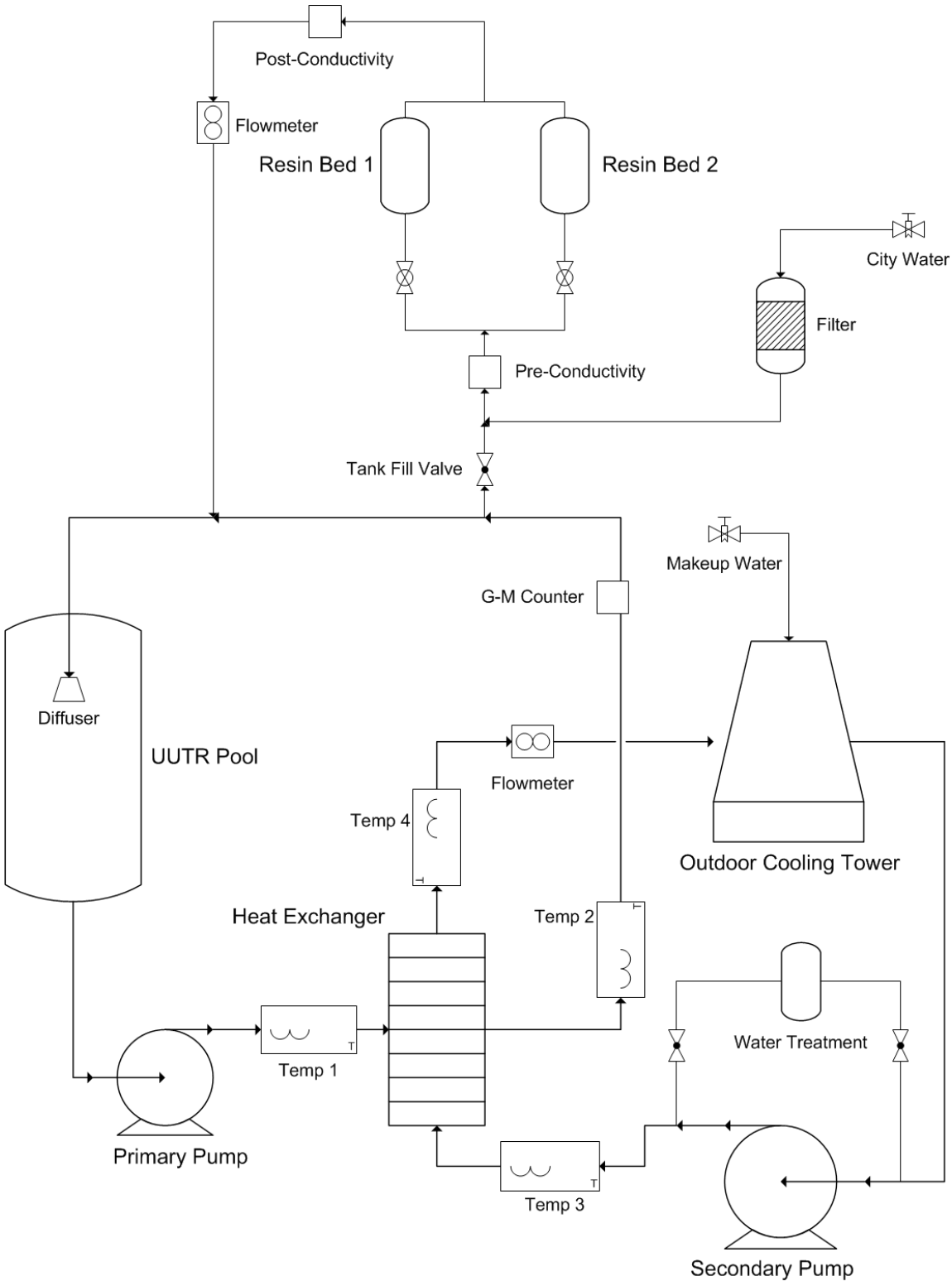

Figure 7-2. Theoritical UUTR Upgraded Cooling System Design

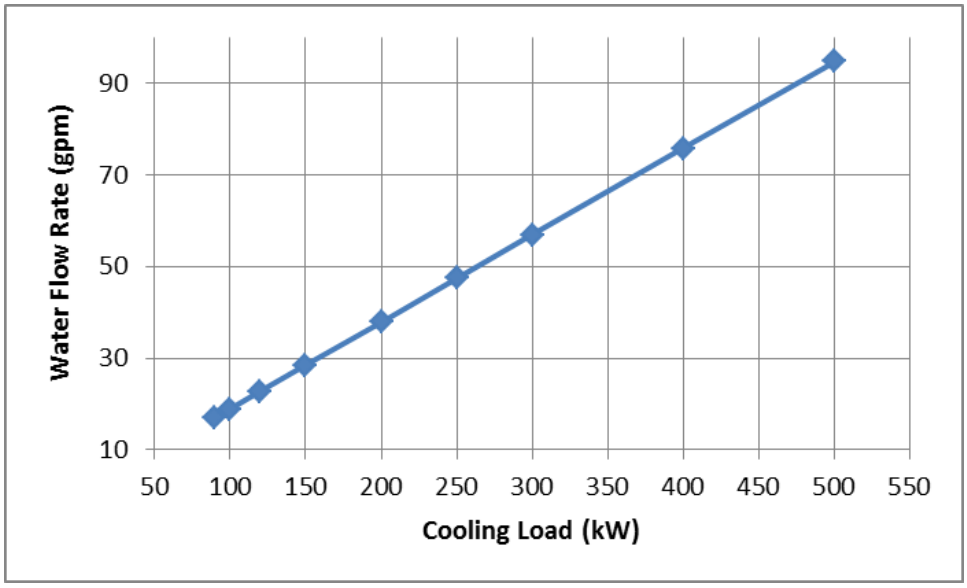

Figure 7-3. Water Flow Rate Required to Maintain a Given Load of Cooling for ΔT=20°C

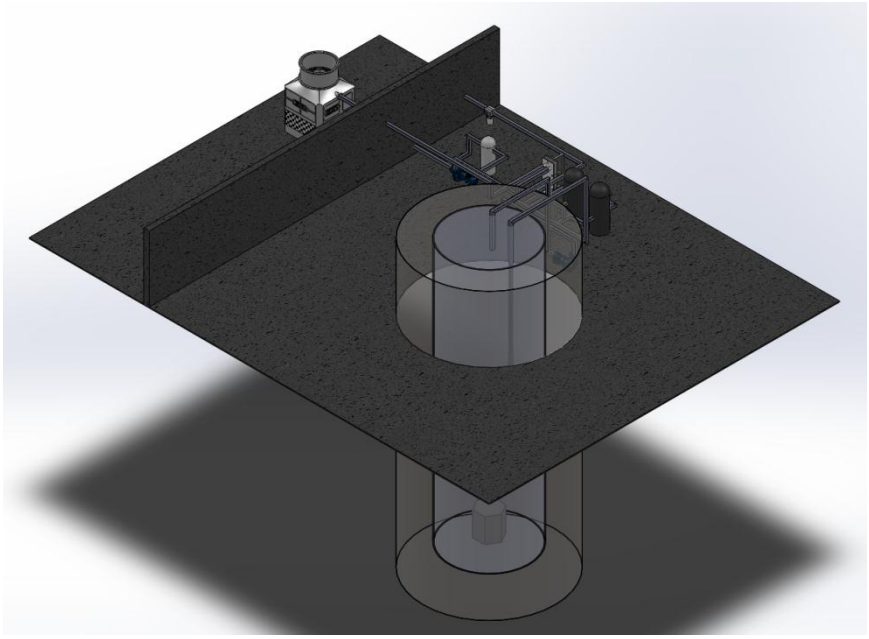

Figure 7-4. Front Isometric View of Theoretical Replacement Cooling System

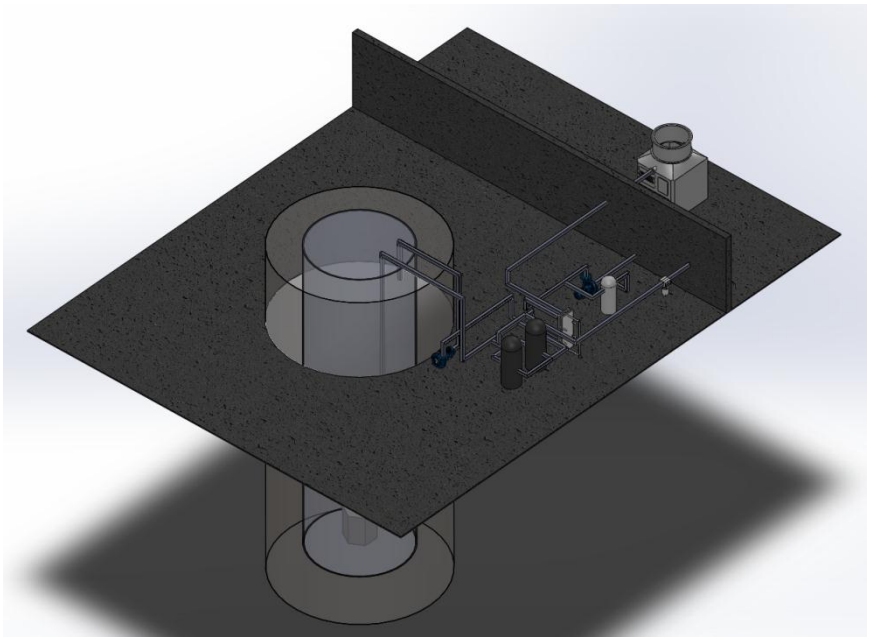

Figure 7-5. Rear Isometric View of Theoretical Replacement Cooling System

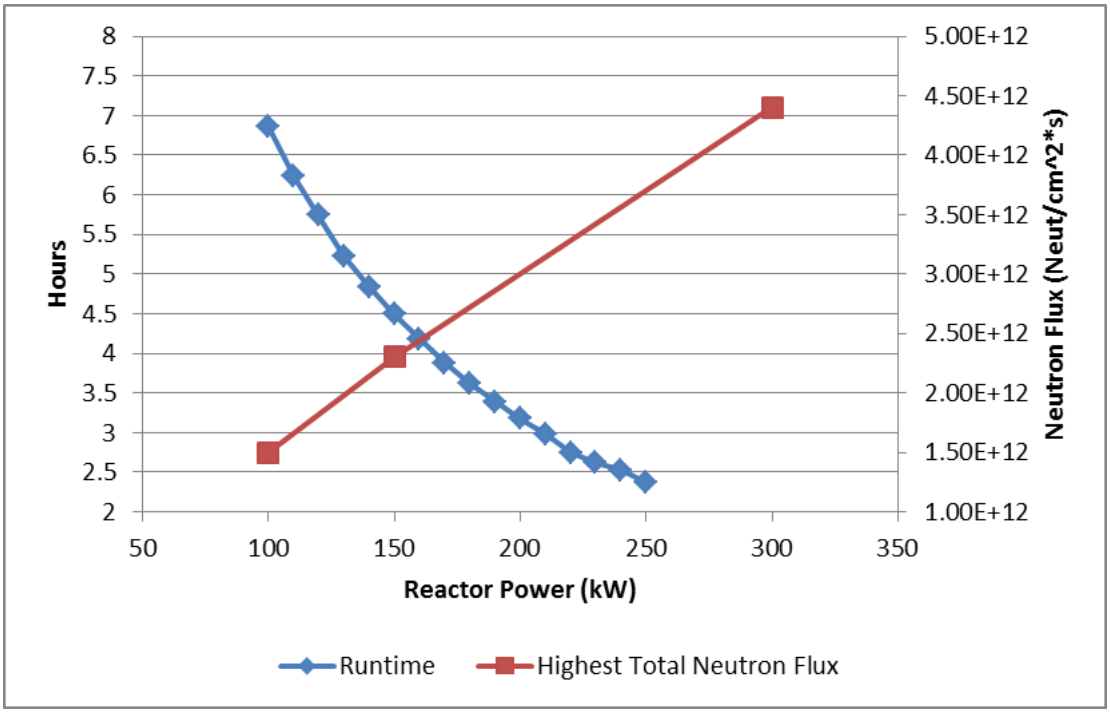

Figure 7-6. UUTR Simulated Runtime and Total Neutron Flux at Varying Power Levels with Pool Temperature Limit of 40°C

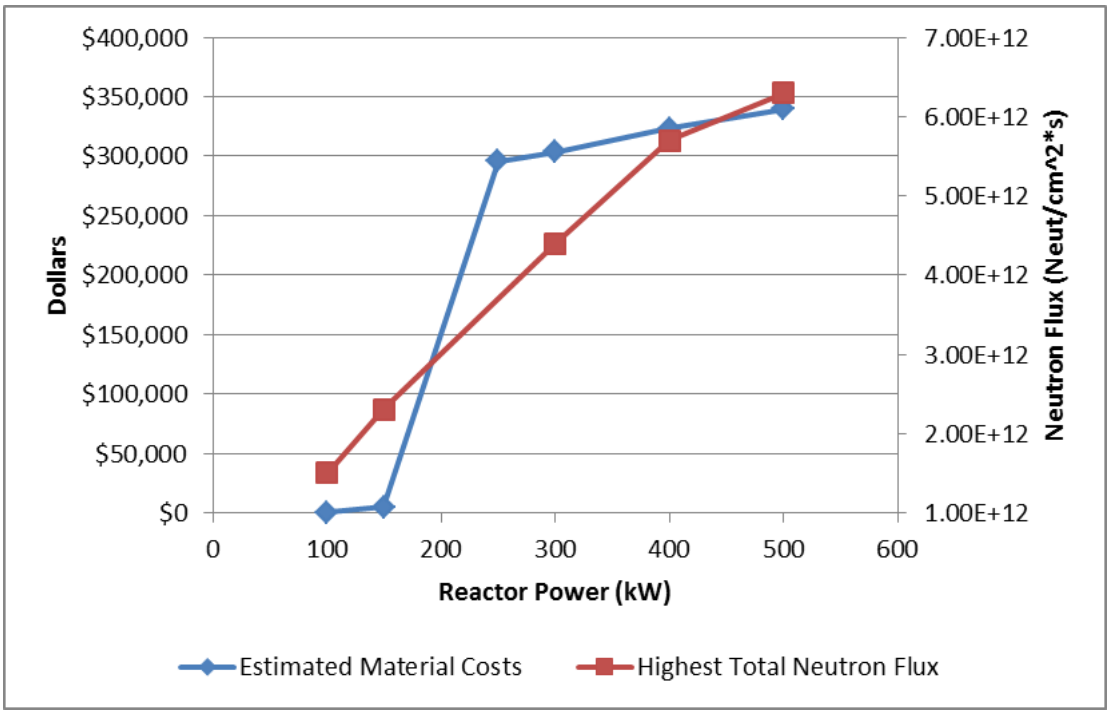

Figure 7-7. UUTR Estimated Power Upgrade Costs and Total Neutron Flux at Varying Power Levels

Table 7-1. Estimated Costs of Cooling System Replacement

Component	Cost
5 hp Centrifugal Pumps (2)	$3,000
S.S. Pipe, Sch. 40, 3" (90 feet)	$5,000
Other Plumbing Components	$1,000
Plate Heat Exchanger (250 kW)	$20,000
Cooling Tower (300 kW)	$50,000
Water Treatment System	$5,000
Temperature Probes (4)	$1,000
Flow Meters (2)	$1,000
G-M Detector	$2,000
Concrete Pad for Cooling Tower	$5,000
Second Mixed Resin Bed	$5,000
Other Construction Materials	$2,000
Cost of Labor (800 man-hours @ $100/hour)	$80,000
Total	**$180,000**

CHAPTER 8

CONCLUSION AND FUTURE WORK

8.1 Conclusion

The objectives of this thesis were to analyze the thermohydraulics aspects of increasing UUTR's power and determine a design basis area for this upgrade with a cost estimate. This was done by first conducting a survey of research reactors and their cooling systems. Simulations of reactor pool conditions were completed using SolidWorks Flow Simulation and Ansys Fluent. 3-D models of the UUTR core and pool were created in each with the flow conditions and temperatures being simulated. An analysis of the departure from nucleate boiling in UUTR was carried out using the PARET-ANL code. The results from these simulations form a basis for a power upgrade to UUTR. Based on these results two potential upgrades were proposed: a low cost upgrade for extended operations was quoted for $5,000 while materials for a complete system replacement that would allow continuous reactor operations were estimated starting at $180,000.

8.2 Recommendations for Future Work

The simulations in Flow Works and Fluent provide insight into UUTR pool conditions at higher powers. These models include the entire reactor pool with a simpler version of the core. The next step using these simulations would be a

higher detail model of the UUTR core without including the surrounding pool. This would allow each individual fuel channel to be modeled and the flow through each to be simulated. These results could then be compared to the hot and nominal channel results from the PARET-ANL code. This would help more accurately determine the DNBR and plan for an ideal future higher power for UUTR.

APPENDIX A

UUTR THERMAL POWER CALIBRATION DATA

Table A-0-1. Historical UUTR Thermal Power Calibration Data (at 90 kW) [Data from 7]

Date	Q_{evap} (J)	Q_{cap} (J)	Time (s)	Q_{evap} (kW)
2/17/06	24,098,529	7.06×10^8	8,460	2.85
8/29/06	23,815,614	7.69×10^8	9,144	2.60
2/23/07	28,490,807	9.81×10^8	10,980	2.59
9/4/07	18,531,387	8.06×10^8	9,241	2.01
1/31/08	21,418,230	6.80×10^8	8,160	2.62
2/26/08	27,357,656	7.66×10^8	9,000	3.04
8/28/08	17,936,497	6.66×10^8	7,632	2.35
2/26/09	17,623,938	6.66×10^8	7,560	2.33
8/27/09	18,778,191	8.16×10^8	9,420	1.99
12/22/09	17,162,425	7.29×10^8	8,399	2.04
2/22/10	30,990,659	1.27×10^9	14,580	2.13
8/20/10	27,165,997	8.49×10^8	10,033	2.71
2/25/11	46,490,336	9.53×10^8	10,800	4.30

APPENDIX B

SOLIDWORKS FLOW SIMULATION LIST OF INPUT PARAMETERS

SolidWorks Flow Simulation Complete List of Input Parameters for 90 kW
General Settings
Analysis Type, Internal
- Exclude cavities without flow conditions, -
- Exclude internal space, -

- Physical Features
- Heat Conduction in Solids, -
- Radiation, -
- Time Dependent, yes
- Gravity, yes
  - X component, 0
  - Y component, -9.81
  - Z component, 0
- Rotation, -
- Reference Axis, X

Fluids
- Project Fluids
- Water (liquid), yes

- Flow Type, Laminar and Turbulent
- Cavitation, -

Wall Conditions
- Default Wall Thermal Condition, Wall Temperature
  - Wall Temperature, 20.00
- Roughness, 0 μm

Initial Conditions
- Thermodynamic Parameters
  - Pressure, 101325
  - Pressure Potential, yes
  - Temperature, 20.00
- Velocity Parameters
  - Velocity in X direction, 0
  - Velocity in Y direction, 0
  - Velocity in Z direction, 0
- Turbulence Parameters
  - Turbulence Intensity, 0.1%
  - Turbulence Length, 0.02229612 m

Computational Domain
3D Simulation
- Xmax, 1.09794751 m
- Xmin, -1.09794751 m

Ymax, 7.31997012 m
Ymin, -0.00477012 m
Zmax, 1.09794751 m
Zmin, -1.09794751 m

Boundary Conditions
Al-vessel, Real Wall
Wall Heat Transfer Coefficient, -177 W/m^2/K
Define Fluid Temperature, Interpolated
Dynamic Boundary Layer Thickness, 0
Adjust Wall Roughness, 0 µm

Heat Sources
Al-core, Heat Source, Surface Source, Face<1>@Al-core-1, Face<2>@Al-core-1, Face<3>@Al-core-1, Face<4>@Al-core-1, Face<5>@Al-core-1, Face<6>@Al-core-1, Face<7>@Al-core-1, Face<8>@Al-core-1
Reference Axis, X
Toggle, Always On
Heat Transfer Rate, Q=90000

Goals
Global Goal
Temperature (Fluid)
Average value
Use for convergence control, yes
Global Goal
Velocity (X)
Minimum value
Global Coordinate System
Use for convergence control, yes
Global Goal
Velocity (Y)
Maximum value
Global Coordinate System
Use for convergence control, yes

Calculation Control Options
Finish
Finish Conditions, If one is satisfied
Minimum refinement number, yes, 1
Maximum iterations, -
Maximum physical time, 21600 s
Maximum calculation time, -
Maximum travels, -
Goals Convergence, -
Refinement
Refinement level, 1
Approximate maximum cells, yes, 2000000
Refinement strategy, tabular
Units, travels
Relaxation interval, auto
Saving
Save before refinement, yes
Periodic saving, yes
Units, physical time (s)
Start, 0 s
Period, 3600 s
Tabular saving, -
Advanced
Calculate LMA, -
Calculate comfort parameters, -
Manual time step, -
Flow Freezing, disabled

APPENDIX C

FLUENT SIMULATION LIST OF INPUT

PARAMETERS AND SETTINGS

Fluent UUTR 250 kW (steady state) Thermohydraulic Simulation
Philip Babitz
Check Mesh

General
- Solver
  - Type; Pressure-Based
  - Velocity Formulation; Absolute
  - Time; Transient
- Gravity; Enabled
  - Gravitational Acceleration
  - X; 0
  - Y; -9.81
  - Z; 0

Models
- Multiphase; off
- Energy; on
- Viscous; laminar
- Radiation; off
- Heat Exchanger; off
- Species; off
- Discrete Phase; off
- Solidification and Melting; off
- Acoustics; off

Materials
- Fluid; Water-liquid
  - Properties
    - Density; boussinesq, 998.2
    - Cp; constant, 4183
    - Thermal Conductivity; constant, 0.6
    - Viscosity, constant; 0.001003
    - Thermal Expansion Coefficient; constant, 0.000207
- Solid; aluminum
  - Properties
    - Density; constant, 2719
    - Cp; constant, 871
    - Thermal Conductivity; constant, 202.4

Cell Zone Conditions
- water-liquid
  - Type; fluid
  - ID; 2
    - Material name; water-liquid
    - Porous zone; off
    - Source terms; off
    - Fixed valus; off
    - Motion Type; stationary

Rotation axis origin; X=0, Y=0, Z=0
Rotation axis direction; X=0, Y=0, Z=1
Operating Conditions
Operating pressure; 101325
Reference pressure location; X=0, Y=0, Z=0
Gravity; on
Gravitational acceleration; X=0, Y=-9.81, Z=0
Boussinesq parameters
Operating temperature; 293
Boundary Conditions
bottom_wall_ab_ring
Type; wall
ID; 20
Momentum
Wall Motion; stationary
Shear Condition; no slip
Thermal
Heat Flux
Heat Flux=0, constant
Wall thickness; 0
Heat generation rate; 0
Material name; aluminum

bottom_wall_c_ring
Type; wall
ID; 21
Momentum
Wall Motion; stationary
Shear Condition; no slip
Thermal
Heat Flux
Heat Flux=0, constant
Wall thickness; 0
Heat generation rate; 0
Material name; aluminum

bottom_wall_d_ring
Type; wall
ID; 22
Momentum
Wall Motion; stationary
Shear Condition; no slip
Thermal
Heat Flux
Heat Flux=0, constant
Wall thickness; 0
Heat generation rate; 0
Material name; aluminum

bottom_wall_e_ring
Type; wall
ID; 23
Momentum
Wall Motion; stationary
Shear Condition; no slip
Thermal
Heat Flux
Heat Flux=0, constant
Wall thickness; 0
Heat generation rate; 0
Material name; aluminum

bottom_wall_f_ring
Type; wall
ID; 24
Momentum
Wall Motion; stationary

Shear Condition; no slip
Thermal
Heat Flux
Heat Flux=0, constant
Wall thickness; 0
Heat generation rate; 0
Material name; aluminum

bottom_wall_g_ring
Type; wall
ID; 25
Momentum
Wall Motion; stationary
Shear Condition; no slip
Thermal
Heat Flux
Heat Flux=0, constant
Wall thickness; 0
Heat generation rate; 0
Material name; aluminum

bottom_wall_ring
Type; wall
ID; 5
Momentum
Wall Motion; stationary
Shear Condition; no slip
Thermal
Convection
Heat transfer coefficient=920, constant
Free stream temperature=295, constant
Wall thickness; .75 in
Heat generation rate; 0
Material name; aluminum

interior_water
Type; interior
ID; 1

side_core_wall_10
Type; wall
ID; 19
Momentum
Wall Motion; stationary
Shear Condition; no slip
Thermal
Heat Flux
Heat Flux=375138, constant
Wall thickness; 0
Heat generation rate; 0
Material name; aluminum

side_core_wall_2
Type; wall
ID; 14
Momentum
Wall Motion; stationary
Shear Condition; no slip
Thermal
Heat Flux
Heat Flux=287880, constant
Wall thickness; 0
Heat generation rate; 0
Material name; aluminum

side_core_wall_3
Type; wall

ID; 15
Momentum
Wall Motion; stationary
Shear Condition; no slip
Thermal
Heat Flux
Heat Flux=279673, constant
Wall thickness; 0
Heat generation rate; 0
Material name; aluminum

side_core_wall_5
Type; wall
ID; 16
Momentum
Wall Motion; stationary
Shear Condition; no slip
Thermal
Heat Flux
Heat Flux=344649, constant
Wall thickness; 0
Heat generation rate; 0
Material name; aluminum

side_core_wall_7
Type; wall
ID; 17
Momentum
Wall Motion; stationary
Shear Condition; no slip
Thermal
Heat Flux
Heat Flux=379616, constant
Wall thickness; 0
Heat generation rate; 0
Material name; aluminum

side_core_wall_9
Type; wall
ID; 18
Momentum
Wall Motion; stationary
Shear Condition; no slip
Thermal
Heat Flux
Heat Flux=513023, constant
Wall thickness; 0
Heat generation rate; 0
Material name; aluminum

side_water_wall
Type; wall
ID; 6
Momentum
Wall Motion; stationary
Shear Condition; no slip
Thermal
Convection
Heat transfer coefficient=920, constant
Free stream temperature=295, constant
Wall thickness; .75 in
Heat generation rate; 0
Material name; aluminum

top_wall_ab_ring
Type; wall
ID; 8

Momentum
Wall Motion; stationary
Shear Condition; no slip
Thermal
Heat Flux
Heat Flux=427421, constant
Wall thickness; 0
Heat generation rate; 0
Material name; aluminum

top_wall_c_ring
Type; wall
ID; 9
Momentum
Wall Motion; stationary
Shear Condition; no slip
Thermal
Heat Flux
Heat Flux=387723, constant
Wall thickness; 0
Heat generation rate; 0
Material name; aluminum

top_wall_d_ring
Type; wall
ID; 10
Momentum
Wall Motion; stationary
Shear Condition; no slip
Thermal
Heat Flux
Heat Flux=290095, constant
Wall thickness; 0
Heat generation rate; 0
Material name; aluminum

top_wall_e_ring
Type; wall
ID; 11
Momentum
Wall Motion; stationary
Shear Condition; no slip
Thermal
Heat Flux
Heat Flux=291515, constant
Wall thickness; 0
Heat generation rate; 0
Material name; aluminum

top_wall_f_ring
Type; wall
ID; 12
Momentum
Wall Motion; stationary
Shear Condition; no slip
Thermal
Heat Flux
Heat Flux=202471, constant
Wall thickness; 0
Heat generation rate; 0
Material name; aluminum

top_wall_g_ring
Type; wall
ID; 13
Momentum
Wall Motion; stationary

Shear Condition; no slip
Thermal
Heat Flux
Heat Flux=25275, constant
Wall thickness; 0
Heat generation rate; 0
Material name; aluminum

top_water_wall
Type; wall
ID; 7
Momentum
Wall Motion; stationary
Shear Condition; no slip
Thermal
Convection
Heat transfer coefficient=0, constant
Free stream temperature=295, constant
Wall thickness; 0
Heat generation rate; 0
Material name; aluminum

Dynamic Mesh; off

Reference Values
Area; 1
Density; 1.225
Enthalpy; 0
Length; 39.37008
Pressure; 0
Temperature; 288.16
Velocity; 1
Viscosity; 1.7894e-05
Ratio of specific heats; 1.4
Reference zone; water

Solution Methods
Scheme; PISO
Skewness correction; 1
Neighbor correction; 1
Skewness-neighbor coupling; on
Spatial Discretization
Gradient; least squares cell based
Pressure; second order
Momentum; first order upwind
Energy; first order upwind
Transient Formulation; first order implicit
Non-iterative time advancement; off
Frozen flux formulation; off

Solution Controls
Under-relaxation Factors
Pressure; 0.3
Density; 1
Body forces; 1
Momentum; 0.7
Energy; 1

Monitors
Residuals; print, plot
Statistic; off
Drag; off
Lift; off
Moment; off

Solution Initialization
Reference Frame; relative to cell zone

- Initial Values
  - Gauge Pressure; 0
  - X velocity; 0.002
  - Y velocity; 0.01
  - Z velocity; 0.002
  - Temperature; 293

Calculation Activities
- Autosave timesteps; 300
- Solution animations; 2
  - Temp; 300, s, x-center
  - Vel; 300, s, x-center

Run Calculation
- Time step; fixed
- Time step size; 1
- Number of time steps; 3600
- Max iterations/time step; 700
- Reporting interval; 10
- Profile update interval; 10

Calculate

APPENDIX D

PARET-ANL INPUT CODE

```
*PARET:  The University of Utah TRIGA Reactor: 150kW (Steady State)
1001,    -2    19     7     1     0     1
1002,     0     0     6    -1     0    20
1003,    1.5-1       0.032540    1.66339+5 -20.60        1.79200-2
1004,    1.74110-2   1.74200-2   0.0         0.0         0.3810     0.1016
1005,    0.1016      0.0078     27.900-6   9.80664     0.00679
1006     0.00        0.80        1.0       998.63      -0.47296
1007,   -2.02010-3   1.15817-5   0.00        0.00        1.00       0.001
1008,    0.00        0.001       0.001       0.05        0.05       0.05
1009,    1.4         0.33
1111,    0.039556    1.00         1.00
1112,     0     1     1     6     1     0
1113,    3.81         0.2       10000.0      0.00
1114,   6.7056       0.6096
2001,    0.0         0.0        18.00        0.00        0.00
2002,    0.0         0.4170+4    2.0400+6    0.00       -273.0
2003,    0.0         0.0         0.199000    0.00        0.00
2004,    0.0         0.0         6.66340+2   0.00        0.00
2005,    0.0         0.0        16.8         0.00        0.00
2006,    0.0         0.0         3.975+6     0.00        0.00
3001,   4.35275-3     5     1   0.980
3002,    9.0-6        6     2   0.000
3003,    5.00-4       7     3   0.000
4001,    0.02005     19
5100,     1     0  0.02794     0.007874    0.5         0.55       1.0
5100,    1.00        0.00        0.00
5101,    0.6096     6.7056       4.38511-2   4.38511-2  1.3818      1.250
5102     1.0988      1.00        1.00        1.00
5103,    1.1244      1.00        1.00        1.00
5104,    1.2662      1.00        1.00        1.00
5105,    1.4256      1.00        1.00        1.00
5106,    1.5657      1.00        1.00        1.00
5107,    1.6921      1.00        1.00        1.00
5108,    1.7812      1.00        1.00        1.00
5109,    1.8524      1.00        1.00        1.00
5110,    1.8965      1.00        1.00        1.00
5111,    1.9373      1.00        1.00        1.00
5112,    1.8960      1.00        1.00        1.00
5113,    1.8515      1.00        1.00        1.00
5114,    1.7789      1.00        1.00        1.00
5115,    1.6881      1.00        1.00        1.00
5116,    1.5595      1.00        1.00        1.00
5117,    1.4162      1.00        1.00        1.00
5118,    1.2536      1.00        1.00        1.00
5119,    1.1078      1.00        1.00        1.00
5120,    1.0797      1.00        1.00        1.00
5200,     1     0  0.02794     0.992126     0.5         0.55        1.00
5200,    1.00        0.0         0.0
5201,    0.6096     6.7056       4.38511-2   4.38511-2 1.3818       1.250
```

```
5202,   0.8326     1.00       1.00       1.00
5203,   0.8387     1.00       1.00       1.00
5204,   0.9198     1.00       1.00       1.00
5205,   0.9991     1.00       1.00       1.00
5206,   1.0696     1.00       1.00       1.00
5207,   1.1580     1.00       1.00       1.00
5208,   1.2090     1.00       1.00       1.00
5209,   1.2493     1.00       1.00       1.00
5210,   1.2808     1.00       1.00       1.00
5211,   1.2979     1.00       1.00       1.00
5212,   1.2794     1.00       1.00       1.00
5213,   1.2465     1.00       1.00       1.00
5214,   1.2047     1.00       1.00       1.00
5215,   1.1520     1.00       1.00       1.00
5216,   1.0616     1.00       1.00       1.00
5217,   0.9891     1.00       1.00       1.00
5218,   0.9077     1.00       1.00       1.00
5219,   0.8245     1.00       1.00       1.00
5220,   0.8161     1.00       1.00       1.00
9000,    2
9001,   1.0-1      0.000      1.0-1       0.15
10000,   2
10001,  158.00      0.00      158.00      1000.00
11000,   2
11001,  0.0       10.00       0.5       1000.0
12000,   2
12001,  5978.13       0.0     5978.13     1000.0
14000,   6
14001,  0.001     0.0        0.0001     0.20        0.00005    0.25
14002,  0.0005    0.28       0.001      1.00        0.005      1.50
16000,   6
16001,  0.1         50       0.0        0.02         10        0.20
16002,  0.005        1       0.25       0.10         10        0.28
16003,  0.50        25       1.00       1.00         10        1.50
17000,   2
17001,  1.0         0.0      1.00000   455.0
18000,   2
18001,  0.0         0.0     -4.00       0.381
```

REFERENCES

1. University of Utah Department of Nuclear Engineering. *UUTR Safety Analysis Report*; NRC Document #ML10321004; NRC: Rockville, MD, 2011.

2. Nuclear Regulatory Commission. Map of Research and Test Reactor Sites. http://www.nrc.gov/reactors/operating/map-nonpower-reactors.html (accessed March 29, 2012).

3. Jevremovic, T. *Nuclear Principles in Engineering*, 2nd Ed.; Ch. 5; Springer Science and Business Media: New York, 2008.

4. Kim, S.H.; El-Genk, M.S.; Rubio, R.A.; Bryson, J.W.; Foushee, F.C. In *Heat Transfer Experiments and Correlations for Natural and Forced Circulations of Water in Rod Bundles at Low Reynolds Numbers*. U.S. TRIGA Users Conference, Washington D.C., April 1988.

5. Feldman, E.E. *Fundamental Approach to TRIGA Steady-State Thermal-Hydraulic CHF Analysis*; Argonne National Laboratory, Nuclear Engineering Division: Argonne, December 2007.

6. Cengel, Y.; Boles, M. *Thermodynamics an Engineering Approach,* 6th Ed.; Property Tables and Charts; McGraw Hill: Boston, 2008.

7. Utah Nuclear Engineering Program. *Thermal Power Calibration and Logs*; UNEP-012; UNEP: Salt Lake City, UT, 2006 – 2011.

8. Incropera, F.; Dewitt, D.; Bergman, T.; Lavine, A. *Fundamentals of Heat and Mass Transfer*, 6th Ed.; Ch. 3, Ch. 9, Ch. 10; John Wiley and Sons: New Jersey, 2007.

9. SolidWorks, verison 2011 with Flow Simulation package; Dassault Systèmes SolidWorks Corporation: Waltham, MA, 2011.

10. SolidWorks Corporation. Driving Better Product Design with SolidWorks Simulation. http://www.solidworks.com/sw/wp-driving-product-design-with-simulation.htm (accessed July 20, 2012).

11. SolidWorks Corporation. *Flow Simulation 2010 Technical Reference*; SolidWorks Corporation, Waltham, MA, 2010.

12. Computational Fluid Dynamics Online. Favre Averaged Navier-Stokes Equations. http://www.cfd-online.com/Wiki/Favre_averaged_Navier-Stokes_equations (accessed July 25, 2012).

13. Ansys Workbench, version 12.1 with Fluent software; Ansys Inc.: Canonsburg, PA, 2011.

14. Ansys Inc. *Ansys Fluent Theory Guide,* Release 14.0; Ch.1, Ch.5; Ansys Inc.: Canonsburg, PA, November, 2011.

15. Ansys Inc, *Ansys Fluent User's Guide*, Release 13.0; Ch.14; Ansys Inc.: Canonsburg, PA, November, 2010.

16. Cutic, A. Feasibility Study of the University of Utah TRIGA Reactor Power Upgrade in Respect to Control Rod System. Master's Thesis, University of Utah, Salt Lake City, UT, 2012.

17. Woodruff, W.L.,; Smith, R.S. *PARET-ANL: Code System to Predict Consequences of Nondestructive Accidents in Research and Test Reactor Cores*; Argonne National Laboratory: Argonne, March, 2001. Provided by Radiation Safety Information Computational Center.

18. General Dynamics. Annular Core Pulse Reactor. *General Atomic Division Report*. GACD 6977, Supplement 2, September 30, 1966.

19. Mesquita, A.; Rezende, H.C. Experimental Heat Transfer Analysis of the IPR-R1 TRIGA Reactor. *Proceedings of the 3rd World TRIGA Users Conference.* Belo Horizonte, Brazil, August 22-25, 2006.

20. Lamarsh, J. R.; Baratta, A.J. *Introduction to Nuclear Engineering,* 3rd Ed.; Ch. 8; Prentice Hall: New Jersey, 2001.

21. International Atomic Energy Agency. *Research Reactor Modernization and Refurbishment;* IAEA TEC-DOC-1625; IAEA: Vienna, Austria, August, 2009.

22. Andrade, V. M. In *Upgrading the IPR-R1 TRIGA Reactor to 250 kW*, European TRIGA Owners Conference, Otaniemi, Helsinki, Finland, 25-27 Aug, 1970.

23. Yazid, P.I.; Kamajaya, K. Upgrade of the Bandung TRIGA 2000 Reactor. *Nuclear Technology Center for Materials and Radiometry*. National Nuclear Energy Agency: Indonesia, August, 2009.

24. Anderson, T.V.; Johnson, A.G. In *Cooling system upgrading from 250 kW to 1 MW*, TRIGA Owners Conference, College Station, TX, 21-22 Feb, 1972.

25. Purolite. Purolite Ion Exchange Resins.http://www.purolite.com (accessed August 22, 2012).

26. ResinTech. ResinTech Inc. http://www.resintech.com/ (accessed August 22, 2012).

27. ResinTech. ResinTech MBD-10. http://resintech.com/products/showfile.aspx?ProductID=78 (accessed August 22, 2012).

28. Water Specialties. Salt Lake City, UT. Telephone Interview, September 5, 2011.

29. McMaster-Carr. Product Catalogue: "Standard-Wall Stainless Steel Threaded Pipe", "Centrifugal Pumps". http://www.mcmaster.com/, (accessed August 23, 2012).

30. Alfa Laval. Richmond, VA. Telephone Interview, August 24, 2012.

31. Mountain States Engineering and Controls. Lakewood, CO. Telephone and E-mail Interview, August 28, 2012.